TÉCNICO LISBOA

Semiclassical approximation for non-Hermitian operators - Application to stochastic optimization

Carlos Alberto Rebelo Couto

Thesis to obtain the Master of Science Degree in

Engineering Physics

Supervisor(s): Prof. José Manuel Vergueiro Monteiro Cidade Mourão
Prof. Pedro José Gonçalves Ribeiro

Examination Committee

Chairperson: Prof. José Pizarro de Sande e Lemos
Supervisor: Prof. José Manuel Vergueiro Monteiro Cidade Mourão
Member of the Committee: Prof. Bruno Miguel Santos Mera

December 2020

Acknowledgments

First of all, I would like to thank both of my supervisors, Professor José Mourão and Professor Pedro Ribeiro, for guiding me throughout my first foray into research. Taking into account the dire world situation during this entire year, I never felt that I lacked neither the support nor the encouragement to progress forward, on either the physical or digital meetings along the year. I also have to extend this acknowledgement to Professor João Pimentel Nunes, who, while not an official supervisor, was always present and eager to contribute to the many interesting discussions that happened across the year.

Secondly, I would like to thank my family, especially my parents, for giving me the opportunity to study what I like and for never doubting in me. This work would not exist without your support.

I extend my deepest gratitude to you, Diana. For always being there for me, sharing my pain and sorrow as well as my joy, no matter the cause. For me to be able to say all of that is the ultimate privilege you have given me. In a way, this work is as much an achievement of mine as is yours. π!

Lastly, I acknowledge the financial support via the project (1801P.00819.1.01) GASonSQuaT-PTDC/MAT-OUT/28784/2017 and also via the project UIDB/04459/2020 from FCT.

Resumo

Nesta tese estudamos a dinâmica semiclássica de sistemas quânticos não-Hermíticos no espaço de fases. A dinâmica semiclássica não Hermitíca de estados coerentes Gaussianos é descrita por um sistema de equações para o movimento do centro e da métrica associada ao pacote de ondas, à qual chamamos a geometria intrínseca do estado. A inclusão de uma parte não Hermítica leva à não conservação da norma, que pode ser interpretada como perda ou ganho de energia. Neste trabalho, propomos um novo método de desacoplar o sistema de equações que simplifica substancialmente o problema. Aplicamos este método a exemplos específicos como a partícula livre em tempo imaginários e o oscilador harmónico em tempo imaginário. Além disso, um método de análise numérica é proposto para integrar a equação de Schrödinger com Hamiltonianos não-Hermíticos. O método é adaptado para a equação de evolução no tempo para a função de Wigner, permitindo então comparar os resultados da aproximação semiclássica com a evolução no tempo de um dado estado inicial, ditado pela equação de Schrödinger. Por fim, uma conexão é feita entre o formalismo de otimização estocástica para uma certa classe de sistemas de controlo e a evolução semiclássica gerada por um Hamiltoniano não-Hermítico quântico. Um exemplo de um Hamiltoniano quadrático é explorado onde mostramos a existência do limite de tempo infinito para o centro e para a métrica do pacote de ondas.

Palavras Chave

Hamiltonianos não-Hermíticos, aproximação semiclássica, método de passo-separado de Fourier, sistemas de controlo estocásticos.

Abstract

In this thesis we study the semiclassical dynamics of non-Hermitian quantum systems on phase space. The non-Hermitian semiclassical dynamics of Gaussian coherent states is described by a system of equations for the motion of the center and of the metric associated with the wave packet, which we call the intrinsic geometry of the state. The inclusion of a non-Hermitian part leads to the non conservation of the norm, which can be interpreted as either energy loss or gain. In this work, we propose a new method of decoupling the system of equations which substantially simplifies the problem. We apply this method to specific examples like the free particle in imaginary time and the harmonic oscillator in imaginary time. Furthermore, a numerical analysis method is proposed for integrating the Schrödinger equation with non-Hermitian Hamiltonians. The method is adapted to the time evolution equation for the Wigner function, thus allowing one to compare the results for the semiclassical approximation with the time evolution of a given initial state, dictated by the Schrödinger equation. Lastly, a connection is made between the formalism of stochastic optimization of a certain class of control systems and the semiclassical evolution generated by a quantum non-Hermitian Hamiltonian. An example of a quadratic Hamiltonian is explored where we show the existence of the infinite time limit of the center and the metric of the wave packet.

Keywords

Non-Hermitian Hamiltonians, semiclassical approximation, split-step Fourier method, stochastic control systems.

Contents

List of Figures

List of Tables

Abbreviations

OQS Open Quantum Systems

NHH Non-Hermitian Hamiltonian(s)

BCH Baker-Campbell-Hausdorff

FT Fourier Transform

DFT Discrete Fourier Transform

FFT Fast Fourier Transform

HJB Hamilton-Jacobi-Bellman

1

Introduction

In Physics, one is usually interested in analyzing a given subsystem of the Universe and such a system is never fully isolated. One often then has to turn to the theory of open quantum systems (OQS) [3]. Nowadays, this theory serves as the backbone to modern research in quantum mechanics and its applications. OQS are very important for example in the fields of quantum information and computation. Here, although results are usually derived using the regular closed system quantum mechanics, one needs models that take into account that a quantum computer is an OQS and may have unwanted interactions that may change the dynamics.

Due to the typically very large amount of degrees of freedom of the environment it is often unfeasible to search for a description of the system plus environment solely based on unitary quantum mechanics. As such, there are several formalisms that try to explain the behavior of OQS and in this work we will focus on the **non-Hermitian Hamiltonian** (NHH) formalism.

One possible way to mimic the behavior of OQS is to consider an effective Hamiltonian that contains an imaginary term used to model the exchange of energy with the environment. This approach is called non-Hermitian quantum mechanics, which is a field that has been attracting a lot of visibility in recent years. The study of NHH raised in interest in 1998, when Carl Bender and Stefan Boettcher showed that PT-symmetric (parity-time symmetric) non-self adjoint Hamiltonians could have real eigenvalues [2]. As such, one does not need to enforce the more restrictive condition of hermiticity to get a real energy spectrum. Since then, examples of such Hamiltonians have been observed in the field of Quantum Optics [17], where new breakthroughs in light-wave dynamics have been devised thanks to the unusual effects that show up when studying NHH. Examples of these applications as well as an introduction to the field of non-Hermitian optics can be found in [10]. However, PT-

symmetric Hamiltonians are just a small subset of the theory of NHH [26]. By extending quantum mechanics to handle NHH one can also shed light into physical processes like resonance phenomena in metastable states or even speed up numerical calculations in unitary quantum mechanics [27]. Furthermore, an emergent field that relies on the study of NHH is topological photonics [31], where topological concepts are used to control the dynamics of light, and NHH play a role as being the source of gain and loss in these optical systems.

One particular area of interest is the semiclassical limit of non-Hermitian dynamics [14–16]. Starting first by studying how NHH behave in the coherent state approximation it has been shown that, for both the state [14], and for the Wigner function of the state [15], one gets a generalized system of equations that describes the phase space evolution of the center of the state and of the associated metric [16]. In a recent work [29], a new method of solving this coupled system of equations has been proposed.

In the present work an equivalence between a class of stochastic optimal control systems and a class of non-Hermitian Hamiltonians has been found. Stochastic control theory has a wide range of applications nowadays, be it in robotics to accurately calculate a robot's course of actions [37] or even in finance, to model the dynamics of financial markets [1]. In particular, for a certain class of control systems it is possible to describe the dynamics of the value function using the formalism developed in this thesis. This study thus shows new methods to simulate and study these controlled systems under a new perspective, that of the non-Hermitian quantum formalism.

The main purpose of this thesis is to explore both numerically and analytically the dynamics and geometry underlying the system of equations that describes the semiclassical dynamics of a non-Hermitian system. Furthermore, we also relate the non-Hermitian formalism to the field of controlled stochastic systems. In the following subsection we introduce the NHH formalism and give some background that will be used later. Following that, we will specify the objectives of this work as well as give an outline of the rest of the thesis.

1.1 Non-Hermitian Hamiltonians

Non-Hermitian Hamiltonians can be regarded as effective Hamiltonians where the imaginary part leads to a certain type of behavior one is attempting to model. Some examples of applications are in OQS, used to mimic the interaction with the environment; in systems with gain and loss like lasers and optical media; and to exhibit finite lifetime in interactions (something that Hermitian quantum mechanics cannot handle) [25]. The move from Hermitian to non-Hermitian dynamics causes several changes which we will briefly mention across this section.

Given a general non-Hermitian Hamiltonian, denoted by $\hat{\mathcal{H}}$, we have that $(\hat{\mathcal{H}} + \hat{\mathcal{H}}^\dagger)/2$ is an Hermitian operator, meaning that it is equal to its conjugate transpose, and that $(\hat{\mathcal{H}} - \hat{\mathcal{H}}^\dagger)/2$ is an anti-Hermitian operator, meaning it is equal to the negative of its conjugate transpose. Moreover, summing the Hermitian operator with the anti-Hermitian operator yields $\hat{\mathcal{H}}$. So, a general non-Hermitian Hamil-

tonian operator can be written as:

$$\hat{\mathcal{H}} = \hat{H} - i\hat{\Gamma}, \tag{1.1}$$

with both $\hat{H}, \hat{\Gamma}$ being Hermitian operators.

If we assume, for simplicity, that the operators are time independent and that $\hat{\mathcal{H}}$ is diagonalizable and has a discrete spectrum then we can always write a general state in the basis of the eigenstates of $\hat{\mathcal{H}}$:

$$|\psi\rangle = \sum_n c_n |\psi_n\rangle , \tag{1.2}$$

with $c_n \in \mathbb{C}$. Furthermore we note that, for a non-Hermitian but diagonalizable $\hat{\mathcal{H}}$, we have:

$$\hat{\mathcal{H}} = \sum_n \mathcal{E}_n |\psi_n\rangle \left\langle \tilde{\psi}_n \right| , \tag{1.3}$$

where, in general, the left and right eigenvectors differ from one another. The fact that left and right eigenvectors may differ from one another follows from the definition of $|\psi_n\rangle$ and $\left\langle \tilde{\psi}_n \right|$:

$$\begin{aligned} \hat{\mathcal{H}} |\psi_n\rangle &= \mathcal{E}_n |\psi_n\rangle \\ \left\langle \tilde{\psi}_n \right| \hat{\mathcal{H}} = \mathcal{E}_n \left\langle \tilde{\psi}_n \right| &\Leftrightarrow \hat{\mathcal{H}}^\dagger \left| \tilde{\psi}_n \right\rangle = \mathcal{E}_n^* \left| \tilde{\psi}_n \right\rangle . \end{aligned} \tag{1.4}$$

From above, we see that the $\left|\tilde{\psi}_n\right\rangle$ are the right eigenvectors of $\hat{\mathcal{H}}^\dagger$ whereas $|\psi_n\rangle$ are the right eigenvectors of $\hat{\mathcal{H}}$. If $\hat{\mathcal{H}}$ was Hermitian then we would have $|\psi_n\rangle = \left|\tilde{\psi}_n\right\rangle$. However, as we are dealing with non-Hermitian Hamiltonians, with complex eigenvalues, we no longer have that equality.

We also have the partition of unity and orthogonality equations for the eigenvectors of the Hamiltonian:

$$\sum_n |\psi_n\rangle \left\langle \tilde{\psi}_n \right| = \mathbb{1} \tag{1.5}$$

$$\left\langle \tilde{\psi}_n \middle| \psi_m \right\rangle = \delta_{nm} \tag{1.6}$$

Having said that, we can deduce the time evolution of such a state, making use of the Schrödinger equation:

$$i\hbar\partial_t |\psi\rangle = \hat{\mathcal{H}} |\psi\rangle \Leftrightarrow \sum_n (\partial_t c_n) |\psi_n\rangle = -\frac{i}{\hbar} \sum_n c_n \mathcal{E}_n |\psi_n\rangle \implies |\psi(t)\rangle = \sum_n c_n e^{-\frac{i}{\hbar}\mathcal{E}_n t} |\psi_n\rangle , \tag{1.7}$$

where $\hat{\mathcal{H}} |\psi_n\rangle = \mathcal{E}_n |\psi_n\rangle$, with $\mathcal{E}_n \in \mathbb{C}$.

The first aspect one notices when studying NHHs is the fact that time evolution is no longer unitary. For example, assuming that the system is initially at the normalized ground state, $|\psi_0(0)\rangle = |\psi_0\rangle$, calculating the norm of the time evolved state one obtains:

$$\langle \psi_0(t) | \psi_0(t) \rangle = e^{-\frac{2}{\hbar}\Gamma_0 t}, \tag{1.8}$$

where $\Gamma_0 = \operatorname{Im} \mathcal{E}_0$. For $\Gamma_0 \neq 0$ this clearly shows an either increasing or decreasing norm for this state.

A particularly useful representation is the Heisenberg picture [9], obtained from Schrödinger's equation and its complex conjugate. For an operator $\hat{A}$ that does not depend explicitly on time, the Heisenberg picture is:

$$i\hbar\partial_t\hat{A}(t) = \left[\hat{A}(t), \hat{H}\right] - i\left\{\hat{A}(t), \hat{\Gamma}\right\} \ , \tag{1.9}$$

where $[.,.]$ denotes the commutator of two operators and $\{.,.\}$ the anticommutator of two operators.

A unique feature of NHH is the existence of singular points, in certain families of Hamiltonians, where both the eigenstates and eigenenergies coalesce [21, 23]. At these points the Hamiltonian is no longer diagonalizable and its eigenvectors no longer span the full Hilbert space. This is different from the usual degeneracy that occurs in Hermitian Hamiltonians because here not only the number eigenvalues but also the number of linearly independent eigenvectors decreases. This is not surprising because the non-Hermitian Hamiltonians may not be diagonalizable.

In this work we will study non-Hermitian Hamiltonians in the semiclassical limit, in which the evolution they generate has an interesting geometric interpretation.

1.2 Objectives

As mentioned above, complex Hamiltonians can be useful tools to study open quantum systems and are an alternative to the more widely studied formalisms like the Lindblad superoperator formalism. Furthermore, as proposed in the present thesis, complex Hamiltonians can also be used in the important field of stochastic control. This approach may shed new light and be more appropriate in certain cases.

The current literature on NHH is able to obtain approximately the semiclassical dynamics of NHH by solving a coupled system of equations for the centers and for the intrinsic geometry of coherent states, proposed in [14–16], which in general is very complicated and computationally expensive. There is another method [29] to approach the system of equations and decouple the equations for the centers from the equation for the geometry, possibly opening up new kinds of systems to be analytically solvable as well as enabling other numerical methods to be used.

Thus, the aim of the present work is to use this aforementioned new method of handling the coupled system of equations in order to model open quantum systems and certain stochastic controlled systems.

Specifically, the objectives are as follows:

- Further exploration of the geometry underlying the system of equations obtained for the coherent state semiclassical evolution generated by NHH in [15, 16];
- Solve the system of equations developed in [15, 16] using the method suggested in [29] in some systems where previously it was not possible to analytically obtain results;
- Find numerical methods to compute solutions of both the exact and semiclassical equations in the context of non-Hermitian Hamiltonians;

- Explore a connection between the fields of stochastic differential equations and non-Hermitian Hamiltonians.

1.3 Thesis outline

In chapter 2, we provide the necessary background to understand the rest of the work. In particular, we introduce the fields of symplectic and Kähler geometry, the Wigner function formalism in the context of coherent states, the system of equations for the semiclassical evolution of a localized state [15, 16] as well as a brief introduction to the field of stochastic control.

In chapter 3, we explore the system of equations proposed in [15, 16] in specific examples and describe their underlying geometry. Furthermore, we also describe a method of handling the system of equations that allows one to analytically solve previously unsolvable examples. Finally, we derive the general equation of motion for the Wigner function for some class of Hamiltonians.

In chapter 4, we present the theoretical background for the numerical methods used to solve the exact evolution equation of a given system as well as their semiclassical evolution according to the equations proposed in [15, 16]. We then apply the method developed in some examples.

Finally in chapter 5, we apply the methods developed beforehand to study a connection between the fields of controlled stochastic differential equations and non-Hermitian Hamiltonians.

2

State of the art

The aim of this chapter is to make a literature review of the topics necessary to the present work. Specifically, we briefly describe Kähler Geometry and the Wigner function formalism. Following that, we describe the system of equations developed in [15, 16] for the motion of the center, the metric and the multiplicative factor of a coherent state. Finally, we end by introducing the field of stochastic optimal control.

2.1 Symplectic and Kähler geometry

Symplectic manifolds [8] provide the natural setting for the Hamiltonian formulation of classical mechanics. They also provide the appropriate setup to study the semiclassical approximation of quantum dynamics. A **symplectic manifold** is a smooth manifold, M, with a closed nondegenerate 2-form ω, called the symplectic form. For the case of classical dynamics on $M = \mathbb{R}^{2n}$ this symplectic form is defined as:

$$\omega = dq \wedge dp = \sum_{j=1}^{n} dq_j \wedge dp_j \tag{2.1}$$

This symplectic form plays a role analogous to the metric in Riemann manifolds. Whereas in Riemann manifolds the metric allows to measure lengths and angles here the symplectic form measures areas of symplectic surfaces in phase space and defines the volume form, called the Liouville form, $\Omega = \omega^n/n!$.

One useful foundational theorem in symplectic geometry is Darboux's theorem, which states that locally we can always find a coordinate system where the symplectic form takes the usual expression

$\omega = dq \wedge dp = \sum_j dq_j \wedge dp_j$. This non unique system of coordinates is called a system of **canonical coordinates**.

Before moving forward we introduce the concept of Hamiltonian vector fields. Given a function from the manifold to the real numbers, $f : M \to \mathbb{R}$, we can obtain a unique vector field X_f, called the Hamiltonian vector field corresponding to f. In canonical coordinates, (p_i, q_i) , this vector field is represented by:

$$X_f = -\sum_{i=1}^{n} \frac{\partial f}{\partial q_i}\frac{\partial}{\partial p_i} + \sum_{i=1}^{n} \frac{\partial f}{\partial p_i}\frac{\partial}{\partial q_i} \,. \tag{2.2}$$

We will need to consider also **complex structures** J on the symplectic manifold (M, ω) [30]. At every point, J is a linear transformation of the tangent space such that $J^2 = -\mathbb{1}_p$, i.e. the identity at point $p \in M$. J is a type $(1, 1)$ tensor field that satisfies an integrability condition $N_J = 0$, with:

$$N_J(X, Y) = [X, Y] + J([JX, Y]) + J([X, JY]) - J([JX, JY]), \tag{2.3}$$

for any vector fields X, Y. Algebraically, this complex structure $J : T_pM \to T_pM$ plays the role of the imaginary unit, where T_pM is the tangent space at p. For example, for vectors tangent to M at p, one can define complex scalar multiplication as $(a + ib)v = av + bJ(v), \forall v \in T_pM$. Note that, for a manifold to have a complex structure, it is required that the manifold is even dimensional. As symplectic manifolds are always even dimensional, that restriction does not pose a problem. Since $J^2 = -\mathbb{1}_p$, it has eigenvalues $\pm i$ that define conjugate eigenspaces of holomorphic and anti-holomorphic directions. In fact, from the holomorphic and anti-holomorphic coordinates, z_j and $\overline{z}_j$, we can define other directions, u_j, v_j from their real and imaginary parts, using the so called Wirtinger derivatives [22]:

$$\begin{aligned} \frac{\partial}{\partial z_j} &= \frac{1}{2}\left(\frac{\partial}{\partial u_j} - i\frac{\partial}{\partial v_j}\right) \\ \frac{\partial}{\partial \overline{z}_j} &= \frac{1}{2}\left(\frac{\partial}{\partial u_j} + i\frac{\partial}{\partial v_j}\right) \,. \end{aligned} \tag{2.4}$$

We can thus also rewrite any vector field, W in this basis

$$W = \sum_{j=1}^{n}\left(W_{u_j}\frac{\partial}{\partial u_j} + W_{v_j}\frac{\partial}{\partial v_j}\right) = \sum_{j=1}^{n}\left(W_{z_j}\frac{\partial}{\partial z_j} + W_{\overline{z_j}}\frac{\partial}{\partial \overline{z_j}}\right) \,. \tag{2.5}$$

The symplectic form and the complex structure are said to be compatible if we require that the complex structure is a symplectic transformation, i.e. iff:

$$\omega\left(Ju, Jv\right) = \omega\left(u, v\right), \forall u, v \in T_pM. \tag{2.6}$$

For the matrix representation of the complex structure on canonical symplectic coordinates this means that $J^T\Omega J = \Omega$ with Ω being the matrix of the symplectic form, defined as:

$$\Omega = \begin{pmatrix} 0 & -\mathbb{1} \\ \mathbb{1} & 0 \end{pmatrix}, \tag{2.7}$$

in the basis (p_j, q_j). For the remainder of the present work we will, unless otherwise stated, always

assume we are in the ordered basis (p_j, q_j).

Note that Eq. (2.6) implies that the tensor g defined as:

$$g(u, v) = \omega(u, Jv), \forall u, v \in T_pM, \tag{2.8}$$

is a symmetric tensor, defined on T_pM. If g is positive definite, i.e a metric, then (M, ω, J, g) is called a **Kähler Manifold** [28]. In a **Kähler Manifold**, the above three structures exist in such a way that they are mutually compatible with each other. Thus, knowing any pair of them allows one to determine the third.

Equivalently, in the matrix representation we have that:

$$G = \Omega J, \tag{2.9}$$

with G being the matrix representation of the metric g, J the complex structure and Ω the symplectic matrix defined above.

2.2 Wigner distribution

In this work we will study non-unitary quantum dynamics in the semiclassical limit. With this goal in mind, we now proceed to briefly introduce the concepts of Gaussian coherent states and their Wigner representation, which serve as a representation of localized states (or wave-packets).

For an harmonic oscillator, a coherent state is defined to be the unique eigenstate of the annihilation operator $\hat{a}$ with associated eigenvalue $\alpha \in \mathbb{C}$. It is a state with minimum uncertainty, that is, it saturates Heisenberg's uncertainty principle. Thus, they are often used as a good bridge between classical and quantum physics.

Since their proposal [13] coherent states have been generalized for arbitrary Lie groups. A good review can be found in Ref. [32]. Here, however, we will only consider coherent states for harmonic oscillators.

An n-dimensional normalized Gaussian coherent state in the Schrödinger representation is defined as:

$$\psi(q) = \frac{(\det \operatorname{Im} B)^{\frac{1}{4}}}{(\pi\hbar)^{\frac{n}{4}}} \exp\left[\frac{i}{\hbar}\left(P \cdot (q - Q) + \frac{1}{2}(q - Q) \cdot B(q - Q)\right)\right], \tag{2.10}$$

where the vector $Y = (P, Q) \in \mathbb{R}^n \times \mathbb{R}^n$ is the center of the state, and the matrix $B \in M_n(\mathbb{C})$ is symmetric, with $\operatorname{Im} B > 0$ to ensure the state is normalizable.

It is possible to pass to a phase space representation of the state using, for example, the Wigner representation [5], originally proposed by Wigner [38]:

$$W(q, p) := \frac{1}{\pi\hbar} \int_{-\infty}^{\infty} dy \psi^*(q + y)\psi(q - y)e^{2ipy/\hbar}. \tag{2.11}$$

The Wigner representation is fundamental to study phase space quantum mechanics. The role

of the Wigner representation is analogous to a probability density function [1] as expectation values for functions of position and momentum can be calculated from it. This is possible because we can obtain both the q and p probability distributions for a pure state from the following integrals:

$$\begin{aligned} |\psi(q)|^2 &= \int_{-\infty}^{\infty} dp W(q,p) \\ \left|\tilde{\psi}(p)\right|^2 &= \int_{-\infty}^{\infty} dq W(q,p) \ , \end{aligned} \tag{2.12}$$

where $\tilde{\psi}(p)$ is the Fourier transform of $\psi(q)$. It worthy of note that, for Gaussian states, the Wigner distribution is always positive and Gaussian. The function is bounded, $-\frac{1}{\pi\hbar} \leq W(q,p) \leq \frac{1}{\pi\hbar}$, but in the limit $\hbar \to 0$ this bound disappears and the Wigner function collapses to the probability density in coordinate space [7].

Its time evolution is given, for an Hamiltonian of the form $\hat{H} = \frac{1}{2m}\hat{p}^2 + V(\hat{q})$ by [5]:

$$\frac{\partial W(p,q,t)}{\partial t} = -\frac{p}{m}\frac{\partial W(p,q,t)}{\partial q} + \sum_{s=0}^{+\infty} \frac{\left(-\hbar^2\right)^s}{(2s+1)!}\left(\frac{1}{2}\right)^{2s} \frac{\partial^{2s+1} V(q)}{\partial q^{2s+1}} \frac{\partial^{2s+1} W(p,q,t)}{\partial p^{2s+1}} \ . \tag{2.13}$$

This approach to quantum mechanics is interesting because it makes quantum mechanics as similar as possible to classical Hamiltonian mechanics. As we will see, in the semiclassical limit we will obtain behavior very similar to the classical Hamiltonian dynamics.

It can be shown that the Wigner function of a Gaussian coherent state of the form of Eq. (2.10) is [15]:

$$W(y) = (\pi\hbar)^{-n} \exp\left[-\frac{1}{\hbar}(y-Y)\cdot G(y-Y)\right], \tag{2.14}$$

where $y = (p,q)$ and $Y = (P,Q)$. The matrix G is obtained from B by:

$$G = \begin{pmatrix} \mathbb{1} & 0 \\ -\operatorname{Re} B & \mathbb{1} \end{pmatrix} \begin{pmatrix} (\operatorname{Im} B)^{-1} & 0 \\ 0 & (\operatorname{Im} B) \end{pmatrix} \begin{pmatrix} \mathbb{1} & -\operatorname{Re} B \\ 0 & \mathbb{1} \end{pmatrix}. \tag{2.15}$$

We note that G is nondegenerate, positive and symmetric and can be seen as describing a constant metric on phase space [15]. Furthermore, it can be seen that it is also a symplectic metric, i.e., $G\Omega G = \Omega$ where Ω is the symplectic structure on phase space defined in Eq. (2.7). Due to this, using Eq. (2.8) it is possible to define a complex structure J, with $J^2 = -\mathbb{1}$ and $\Omega J = G$. Consequently, every coherent state (Eq. 2.10) endows the phase space with a flat **Kähler structure**. Having explained the concepts of non-Hermitian Hamiltonians, coherent states and Kähler geometry we are now in a position to understand the system of equations derived in [15, 16].

2.3 The semiclassical approximation for non-Hermitian Hamiltonians

In their paper on the evolution of wave packets [15] (described by Gaussian coherent states), Graefe and Schubert derive a system of coupled equations for the time evolution of the Wigner func-

[1] It cannot really be a probability density function as it can be negative-valued.

tion of a NHH given by $\hat{\mathcal{H}} = \hat{H} - i\hat{\Gamma}$. They start by inserting a Gaussian ansatz for the time dependent Wigner function:

$$W(t,y) = \frac{\alpha(t)}{(\hbar\pi)^n} \exp\left(-\frac{1}{\hbar}(y - Y(t)) \cdot G(t)(y - Y(t))\right). \tag{2.16}$$

Arriving at the following system of equations for the time dependent parameters $\alpha(t), G(t), Y(t)$:

$$\begin{aligned} \dot{Y} &= \Omega\nabla H(Y) - G^{-1}\nabla\Gamma(Y) \\ \dot{G} &= H''(Y)\Omega G - G\Omega H''(Y) + \Gamma''(Y) - G\Gamma''_\Omega(Y)G, \\ \frac{\dot{\alpha}}{\alpha} &= -\frac{2}{\hbar}\Gamma(Y) - \frac{1}{2}\operatorname{Tr}\left[\Gamma''_\Omega(Y)G\right] \end{aligned} \tag{2.17}$$

where Ω is the usual symplectic matrix as defined in Eq. (2.7), the vector $Y(t)$ is the center of the Wigner wave packet, the metric $G(t)$ which is obtained from the complex matrix $B(t)$ (see Eq. (2.15)), $\Gamma''_\Omega := \Omega^t\Gamma''\Omega$ and the notation A'' denotes the Hessian matrix of $A(y)$ at y.

Notice that the above system of equations is highly coupled and this makes finding its analytical solution difficult except for trivial cases. However, noticing that this evolution takes place in a Kähler manifold, we can rewrite the first dynamical equation for the center of the wave packet using Eq. (2.9):

$$\dot{Y}(t) = \Omega\nabla H(Y) - G^{-1}\nabla\Gamma(Y) = X_H(Y) - J(t)X_\Gamma(Y). \tag{2.18}$$

Notice that J has to depend on time because the metric depends on time and the symplectic structure does not. We see from Eq. (2.18) that, if the Hamiltonian was Hermitian, we would have obtained the classical Hamilton equations as the classical limit for the evolution of these quantum states. However, in the presence of a non-Hermitian term we can see that this evolution no longer corresponds to the flow of a simple Hamiltonian vector field. Instead, the evolution has a component which is mediated by the metric/complex structure. We note that this dependence on the metric for the evolution of the center is unprecedented in unitary quantum mechanics and is an effect only observable when studying NHH.

One important simplification is achieved by decoupling in Eq. (2.17) the equation for the center from the equation for the metric. One rewrites the above equation in terms of functions z that are $J(t)$ holomorphic [29], and for those functions z we have that:

$$\dot{z} = X_H(z) - J(t)X_\Gamma(z) = X_H(z) - iX_\Gamma(z) = X_{\mathcal{H}}(z). \tag{2.19}$$

That is, a equation solely dependent on the time dependent function z. We define ϕ_t from $Y_t = \phi_t(Y_0)$, where $Y(t)$ is the solution of Eq. (2.18). Then, solving equation (2.19) would allow one to obtain the pullback $\phi_t^*(z_0)$ that defines the time evolution for the center $Y(t)$. The pullback $\phi_t^*(z_0)$ is defined from:

$$z_t = z_0 \circ \phi_t = \phi_t^*(z_0)\ . \tag{2.20}$$

Then, using $\phi_t^*(z_0)$ one can calculate the time-dependent complex structure and thus the metric, $G(t)$. Doing so, we are able to obtain the Wigner function $W(p,q,t)$ except for the factor $\alpha(t)$ which can be found by solving the last equation in Eq. (2.17). On subsection 3.3.2, we go into more detail on how

to obtain both the motion of the center as well as the motion of the complex structure, in the two dimensional phase space.

Even in cases which cannot be analytically solved, the above system can be computationally implemented to obtain numerical simulations and results. In the following image we can see a simulation done by Graefe and Schubert [15] on the comparison of the exact numerical propagation of a Wigner function and the semiclassical approximation using Eqs. (2.17). They considered an anharmonic oscillator with damping, with its corresponding Hamiltonian being:

$$\hat{\mathcal{H}} = \left(\frac{1}{2} - i\frac{1}{10}\right)(\hat{p}^2 + \hat{q}^2) + \frac{1}{8}\hat{q}^4 \,, \tag{2.21}$$

and obtained the following figure:

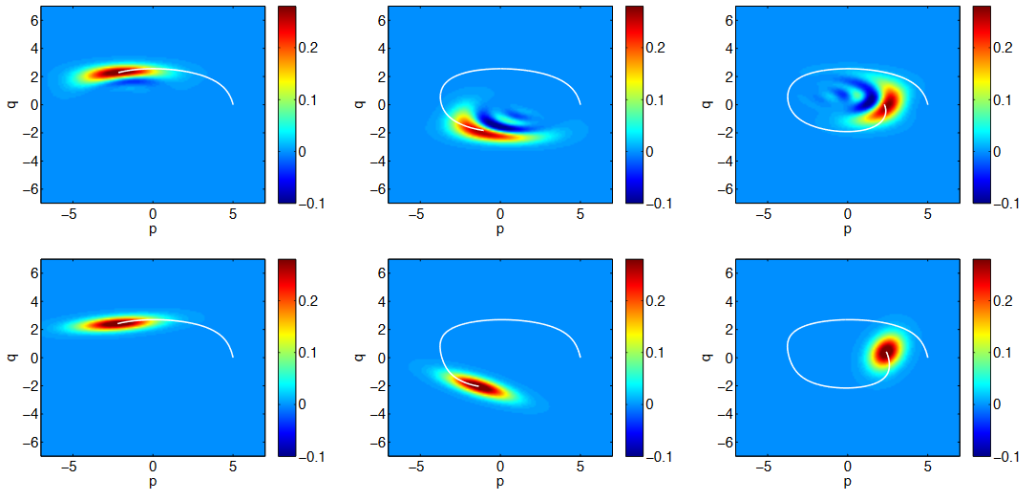

Figure 2.1: Normalized exact Wigner function (top row) versus the semiclassical approximation (bottom row) at different times ($t = 1, 2.5, 4$). The white line shows the motion of the center of the wave packet. Image and simulation done by Graefe et al in [15].

As we can see, on the bottom figure, the semiclassical approximation, which is obtained by solving Eq. (2.17), quite remarkably captures the motion of the center and of the general shape of the localized state, when compared to the respective exact motion, seen on the figures at the top. In particular, we remark that the semiclassical equations (2.17) will always result in a Wigner coherent state. As such, the Wigner function will always be non-negative. Whereas, on the plots at the top, showing the exact numerical propagation under the quartic oscillator, we do see zones where the Wigner function is negative valued.

In the next chapter, we explore this system of equations under specific examples as well as compare both analytical methods of obtaining the solutions for the system. However, before that, we will briefly introduce the field of stochastic differential equations, which will be relevant for chapter 5.

2.4 Stochastic optimal control

2.4.1 Introduction

The field of stochastic optimal control is a branch of optimal control theory. The idea behind optimal control is that, for a given system that can be controlled through some variables, we want to find the optimal choice of control in order to maximize or minimize a given cost function. These systems can range from robotic arms trying to open doors to airplanes trying to lower their fuel consumption by controlling the thrust of the engines.

Stochastic optimal control is the extension of optimal control theory where we take into consideration the fact that both the measurements as well as the control can be affected by noise, which usually takes form of a Gaussian random variable.

In the present section we will study systems whose evolution is described by a stochastic differential equation of the form:

$$\dot{\boldsymbol{x}}_t = \boldsymbol{f}(\boldsymbol{x_t}, \boldsymbol{t}) + \boldsymbol{G}(\boldsymbol{x}_t)\left(\boldsymbol{u}_t + \boldsymbol{\xi}_t\right) \ , \tag{2.22}$$

where $\boldsymbol{x_t} \in \mathbb{R}^n$ is the state of the system, $\boldsymbol{f}(\boldsymbol{x_t}, \boldsymbol{t}) \in \mathbb{R}^n$ describes the passive dynamics, $\boldsymbol{G}(\boldsymbol{x}_t) \in \mathbb{R}^{n\times p}$ is the control matrix, $\boldsymbol{u}_t \in \mathbb{R}^p$ the control variables and finally $\boldsymbol{\xi}_t \in \mathbb{R}^p$ is Gaussian white noise with variance matrix Σ_ξ.

The differential form of the above equation reads:

$$d\boldsymbol{x}_t = \left(\boldsymbol{f}(\boldsymbol{x_t}, \boldsymbol{t}) + \boldsymbol{G}(\boldsymbol{x}_t)\boldsymbol{u}_t\right) dt + \boldsymbol{G}(\boldsymbol{x}_t) d\boldsymbol{W}_t \ , \tag{2.23}$$

where $d\boldsymbol{W}_t$ is a Wiener process. A Wiener process, $\boldsymbol{W}_t$, is a continuous random process such that $\boldsymbol{W}_0 = 0$ and its increments, $\boldsymbol{W}_{t+u} - \boldsymbol{W}_t$, are Gaussian and independent, that is, they are independent of past values of $\boldsymbol{W}_s, s < t$ and they follow a Gaussian distribution with mean 0 and variance u.

For simplification, on the remainder of this section the index t indicates a dependency on the time and state of the system, i.e. $\boldsymbol{u}_t = \boldsymbol{u}(\boldsymbol{x}_t, t)$. Our objective is to optimize a given predefined cost function of the trajectory T_i of the system that at time t_i is in the state $\boldsymbol{x}_{t_i}$ and ends at time t_N in the state $\boldsymbol{x}_{t_N}$. This cost function is defined as:

$$R(T_i) = \phi_{t_N} + \int_{t_i}^{t_N} r_t dt \ , \tag{2.24}$$

where $\phi_{t_N} = \phi(\boldsymbol{x}_{t_N})$ represents a final cost/reward at time t_N and where r_t denotes the instantaneous cost at time t.

The idea of stochastic optimal control is to minimize the above cost function through the control variables $\boldsymbol{u}_t$. We define the value function as the minimum of the expected value of the cost function:

$$V(\boldsymbol{x}_{t_i}) = V_{t_i} = \min_{\boldsymbol{u}_{t_i:t_N}} E_{T_i}[R(T_i)] \ , \tag{2.25}$$

where this expected value is taken over all trajectories that start at $\boldsymbol{x}_{t_i}$.

It can be shown that the value function satisfies the so called Hamilton-Jacobi-Bellman equation

(HJB) [11, 34]:

$$-\partial_t V = \min_{\boldsymbol{u}} \left[r_t + (\partial_{\boldsymbol{x}} V)^T \boldsymbol{F}_t + \frac{1}{2} \operatorname{tr}\left(\left(\partial^2_{\boldsymbol{xx}} V \right) \left(\boldsymbol{G}_t \boldsymbol{\Sigma}_t \boldsymbol{G}_t^T \right) \right) \right] , \tag{2.26}$$

where we have the boundary terminal condition $V(t_N) = E\left[\phi(t_N)\right]$, $\partial_{\boldsymbol{x}} V$ is the gradient vector of V, $\partial^2_{xx} V$ is the Hessian matrix of V and $\boldsymbol{F}_t = \boldsymbol{f}(t, \boldsymbol{x}_t) + \boldsymbol{G}(\boldsymbol{x}_t)\boldsymbol{u}_t$.

As we will see, from the HJB equation (Eq. (2.26)), it is possible to derive an equation similar to the Schrödinger equation for a given class of controlled systems. For a given Hamiltonian the solution of the Schrödinger equation for a Gaussian initial states can be found, in the semiclassical approximation, by solving Eq. (2.17), which yield the motion for the center and the metric associated with the Gaussian state.

2.4.2 Deriving a Schrödinger-like equation from the HJB equation

Following [36], we consider an instantaneous cost of the form:

$$r_t = q(\boldsymbol{x}_t, t) + \frac{1}{2} \boldsymbol{u}_t^T \boldsymbol{R} \boldsymbol{u}_t , \tag{2.27}$$

which has a state dependent part and a quadratic term on the control and where $\boldsymbol{R}$ is a positive definite matrix.

Substituting this cost function in (2.26), taking the gradient of the part we want to minimize with respect to $\boldsymbol{u}_t$ and setting it to zero enables us to get an expression for the optimal control:

$$\boldsymbol{u}(\boldsymbol{x}_t) = -\boldsymbol{R}^{-1} \boldsymbol{G}_t^T \left(\partial_{\boldsymbol{x}} V \right) . \tag{2.28}$$

Moreover we can substitute the expression for the optimal control in the HJB equation (2.26) to get:

$$-\partial_t V = q_t - \frac{1}{2} \left(\partial_{\boldsymbol{x}} V \right)^T \boldsymbol{G}_t \boldsymbol{R}^{-1} \boldsymbol{G}_t^T \left(\partial_{\boldsymbol{x}} V \right) + \left(\partial_{\boldsymbol{x}} V \right)^T \boldsymbol{f}_t + \frac{1}{2} \operatorname{tr}\left(\left(\partial^2_{\boldsymbol{xx}} V \right) \left(\boldsymbol{G}_t \boldsymbol{\Sigma}_t \boldsymbol{G}_t^T \right) \right) , \tag{2.29}$$

which is a second order nonlinear partial differential equation.

By making a change of dependent variable [36]:

$$V_t = -\lambda \log \psi_t , \tag{2.30}$$

as well as using the assumption that $\lambda \boldsymbol{R}^{-1} = \boldsymbol{\Sigma}$ we obtain the following linear equation for ψ:

$$-\partial_t \psi = \frac{1}{2} \operatorname{Tr}\left(\partial^2_{\boldsymbol{xx}} \left(\psi_t \right) \boldsymbol{G}_t \Sigma \boldsymbol{G}_t^T \right) + \boldsymbol{f}_t^T \left(\nabla_x \psi_t \right) - \frac{1}{\lambda} q_t \psi_t , \tag{2.31}$$

with the terminal boundary condition $\psi_{t_N} = \exp\left(-\phi(t_N)/\lambda\right)$. The assumption used is the statement that a high variance control input implies cheap control cost whereas small variance control yields high control cost [36].

By relabeling the parameter $\lambda \to \hbar$ and multiplying (2.31) by $\hbar$ we can see that the above equation has a Schrödinger-like form for a real wave function with a non-Hermitian Hamiltonian associated with

it:

$$-\hbar\partial_t\psi = \frac{1}{2}\hbar^2 \operatorname{Tr}\left(\partial^2_{\boldsymbol{xx}}\left(\psi_t\right)\boldsymbol{G}_t\boldsymbol{R}^{-1}\boldsymbol{G}_t^T\right) + \boldsymbol{f}_t^T\hbar\left(\nabla_x\psi_t\right) - q_t\psi_t \ . \tag{2.32}$$

In chapter 5, we identify the Hamiltonian corresponding to Eq. (2.32) and we study several examples of controlled systems under the NHH formalism.

3

Analytical methods

The aim of the present chapter is to develop the analytical framework to obtain the semiclassical dynamics of non-Hermitian Hamiltonians from the proposed system of equations in [15]. Before that, however, we first discuss the geometry of the squeezed coherent states and its dependence on the parameters of the wave function. Then, we describe the usual way of solving the system, followed by proposing a different way of looking at the system of equations and solving it. We present several examples, using both methods of analytically solving Eq. (2.17). Finally, we derive the partial differential equation for the time evolution of the Wigner function and show it explicitly for some types of Hamiltonians.

3.1 Geometry of the Wigner states in 2-dimensional phase space

In this section we explore, for two dimensional phase space, the geometry of the localized Wigner states which we use on the rest of this work. Specifically, we study how changing the parameters of the wave function alters the resulting Wigner state.

As discussed in the previous chapter, we are dealing with localized Gaussian coherent states which are given, in n-dimensions, by Eq. (2.10). In the two dimensional phase space, the matrix B is a complex number, $B = a + ib\,, a, b \in \mathbb{R}$, whose imaginary part must be positive, $b > 0$. In this space the Wigner function is given by Eq. (2.14) with the matrix G being:

$$G = \begin{pmatrix} \frac{1}{b} & -\frac{a}{b} \\ -\frac{a}{b} & \frac{a^2}{b} + b \end{pmatrix} . \tag{3.1}$$

We can see that G is a real symmetric matrix. In fact, we see that the parameter B naturally induces the metric G, appearing in the expression for the corresponding Wigner function. We can also see that it is positive definite by calculating:

$$y^T G y = \frac{1}{b}\left(y_1 - a y_2\right)^2 + b y_2^2 \, , y \in \mathbb{R}^2 \, , \tag{3.2}$$

and seeing that, as we always have $b > 0$, then we always have $y^T G y > 0, \forall y \in \mathbb{R}^2 \backslash \{0\}$. Furthermore, it also has determinant equal to one. Reciprocally, we can also define the parameter B from just two components of G in the following way:

$$B = a + ib = -\frac{G_{12}}{G_{11}} + \frac{i}{G_{11}} \, . \tag{3.3}$$

Looking at the form for Eq. (2.14), we will now see how the parameters affect the shape of the Gaussian. Without loss of generality, we will consider the Gaussian to be centered at the origin, because the center Y only translates the function across the phase space. If, for example, $B = 2 + i$, we obtain the following plot:

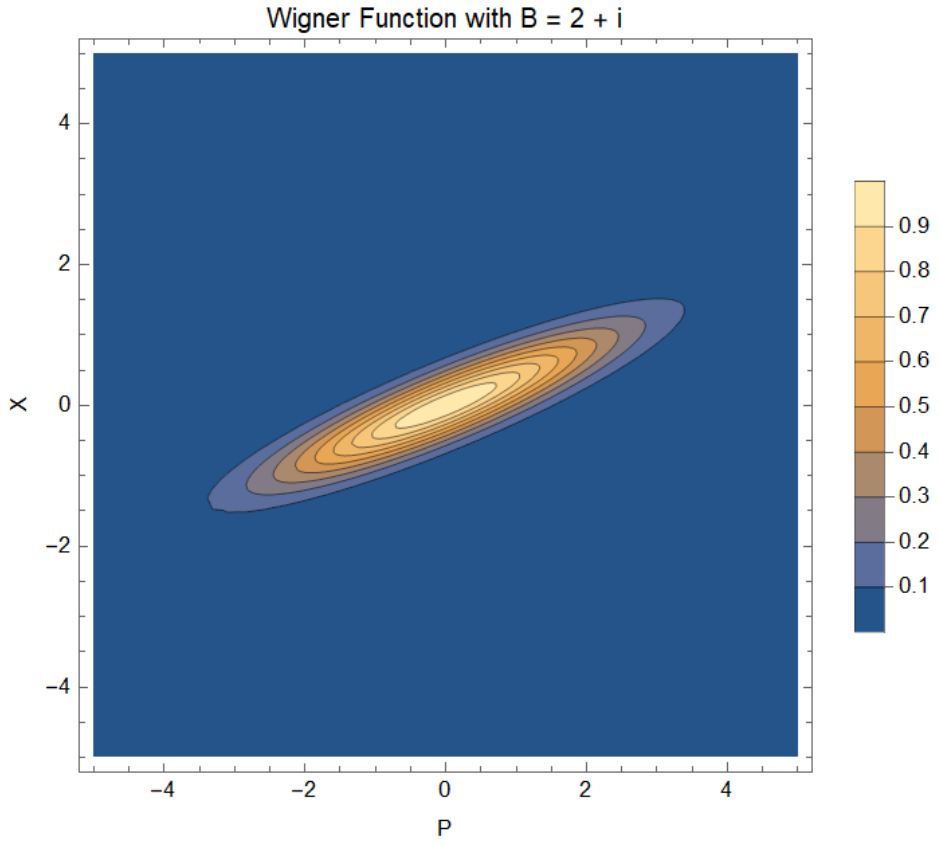

Figure 3.1: Contour plot of the Wigner function, given by Eq. (2.14), when we set $B = 2 + i$.

From Fig. 3.1, we see that the Gaussian function becomes squeezed in a given direction and stretched in another, which appears to be at a $\frac{\pi}{2}$ angle from the former. As G is a symmetric matrix, its eigendecomposition can be given as $G = Q \Lambda Q^{-1}$ where Q is an orthogonal matrix, $Q^{-1} = Q^T$, and Λ is a diagonal matrix with the eigenvalues of G as its components. Furthermore, because G is

also positive definite, we also know that its eigenvalues are all positive. Thus, if we were to write the Wigner state in the eigenbasis we would have:

$$W(y) = (\pi\hbar)^{-n} \exp\left[-\frac{1}{\hbar} y^T Q \Lambda Q^{-1} y\right] = (\pi\hbar)^{-n} \exp\left[-\frac{1}{\hbar} w^T \Lambda w\right] , \tag{3.4}$$

where $w = (w_1, w_2)$ is a vector in the eigenbasis of G. If Λ is ordered by the magnitude of its eigenvalues, from lowest to highest, λ_1, λ_2 then we have:

$$W(w) = (\pi\hbar)^{-n} \exp\left[-\frac{1}{\hbar}\left(\lambda_1 w_1^2 + \lambda_2 w_2^2\right)\right] , \tag{3.5}$$

and so the larger eigenvalue, λ_2, would correspond to the direction of larger squeeze and vice-versa. Moreover, as the determinant of a matrix is invariant under basis transformations, and because $\det G = \lambda_1 \lambda_2 = 1$ we have that $\lambda_1 = \lambda_2^{-1}$. Thus we either have both directions without any squeeze or we have one direction with squeeze with the other one being stretched. If we have a squeezed state then, because Q is orthogonal, the eigenvectors of G are also orthogonal to each other.

It remains to show how the squeezing and angle are related to the parameter $B = a + ib = re^{i\theta}, \theta \in (0, \pi)$. To do that we simply solve the equations for the eigenvalues and eigenvectors to obtain both the smallest eigenvalue, λ, and the angle, α, of the corresponding eigenvector direction. We obtain the following:

$$\begin{aligned} \lambda &= \frac{\csc(\theta)\left(-\sqrt{2r^2\cos(2\theta) + r^4 + 1} + r^2 + 1\right)}{2r} \\ \tan\alpha &= \frac{2r\cos(\theta)}{\sqrt{2r^2\cos(2\theta) + r^4 + 1} + r^2 - 1} \end{aligned} . \tag{3.6}$$

If we plot the expression for λ as a function of r and θ we obtain Fig. 3.2.

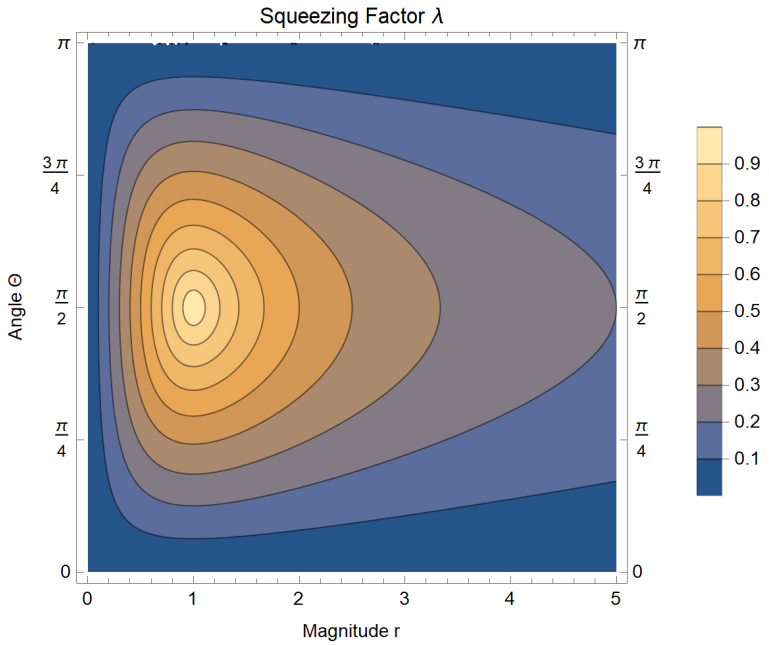

Figure 3.2: Plot of the smallest eigenvalue as a function of the magnitude and angle of the parameter B.

We can see that the value for this eigenvalue ranges from one to zero. Likewise, the other eigenvalue will range from one to infinity. We also plot the tangent of the angle of the eigenvector corresponding to this eigenvalue in Fig. 3.3a. We see that for most values the tangent remains near zero. However, for values of r below one and near $\theta = \frac{\pi}{2}$, we see that the tangent will either tend to positive or negative infinity. On Fig. 3.3b we plot the hyperbolic tangent of Fig. 3.3a in order to see the discontinuity in detail.

Figure 3.3: Plots regarding the tangent of the angle of the eigenvector with the smaller eigenvalue.

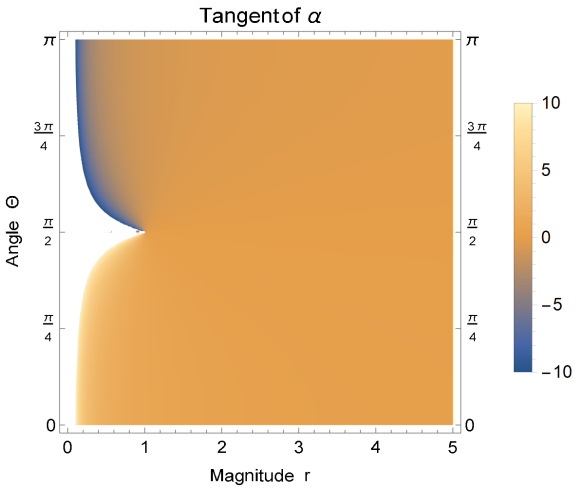

(a) Plot of the tangent of the angle of the eigenvector corresponding to the smaller eigenvalue.

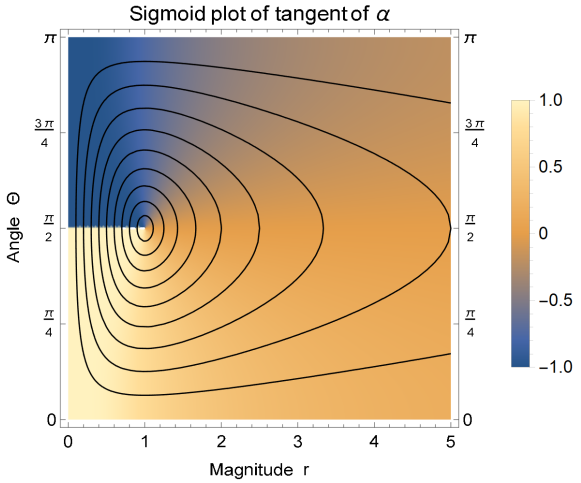

(b) Sigmoid plot of the tangent of the angle of the eigenvector corresponding to the smaller eigenvalue with the contours of Fig. 3.2 on top.

Looking at both Fig. 3.2 as well as Fig. 3.3b, we see that we can obtain any angle for a given value of λ. This is due to the fact that each contour line of λ crosses the discontinuity in the tangent plot. This discontinuity arises when the real part of B crosses zero and the imaginary part is such that $r < 1$. We can see this from the expression for G when $\mathrm{Re}(B) = 0$:

$$G = \begin{pmatrix} \frac{1}{b} & 0 \\ 0 & b \end{pmatrix} . \tag{3.7}$$

From the above we conclude that the momentum direction is the one associated with the $\frac{1}{b}$ eigenvalue meaning that $a = 0, b < 1 \implies r < 1$. Under those assumptions, we see that the smallest eigenvalue is in the position direction, when $\alpha = \frac{\pi}{2}$. When $b > 1$ the smallest eigenvalue is in the momentum direction, where the angle is zero.

3.2 Analyzing the system of equations

Let us analyze the three equations that were proposed in [14–16] to describe the dynamics for a given NHH in the semiclassical approximation. The system was already presented in Eq. (2.17) but for completeness we write it again in order to describe it. Thus the system of equations, for a NHH of

the form $\hat{\mathcal{H}} = \hat{H} - i\hat{\Gamma}$, is as follows:

$$\begin{aligned}
\dot{Y} &= \Omega \nabla H(Y) - G^{-1} \nabla \Gamma(Y) \\
\dot{G} &= H''(Y)\Omega G - G\Omega H''(Y) + \Gamma''(Y) - G\Gamma''_\Omega(Y)G, \\
\frac{\dot{\alpha}}{\alpha} &= -\frac{2}{\hbar}\Gamma(Y) - \frac{1}{2}\operatorname{Tr}\left[\Gamma''_\Omega(Y)G\right]
\end{aligned} \tag{3.8}$$

where Ω is the usual symplectic matrix defined in Eq. (2.7), the vector $Y(t) = (P(t), Q(t))$ is the center of the Wigner wave packet, the metric matrix $G(t)$ is obtained from the initial state matrix B (see Eq. (2.10)) and $\alpha(t)$ is a time-dependent coefficient associated with the initial phase of the Wigner distribution. We also denote by A'' the Hessian matrix of $A(y)$ at y and $\Gamma''_\Omega := \Omega^T \Gamma'' \Omega$.

Upon further inspection of Eq. (3.8), we can see that, for the evolution of the center of the Wigner state, we have a regular Hamiltonian flow for the Hermitian part of the Hamiltonian but with an added contribution from the non-Hermitian part. This contribution from the non-Hermitian part is a gradient flow into the minima of Γ [15]. This implies that, were we to choose Γ with no minima, for example $\Gamma = -q^2 - p^2$, then the anti-Hermitian term would drive the motion of the localized state away from the origin and exponentially so. As for the metric, we see that its evolution equation depends on the center $Y(t)$, making this equation coupled if the Hamiltonian is not quadratic. Lastly, for the coefficient $\alpha(t)$, we can see that its magnitude will in general no longer be unitary and this corresponds either to an increase or decrease in the overall probability due to the non-Hermitian term of the NHH. This is further corroborated by the fact that the dynamics of $\alpha(t)$ only depend on Γ and has no dependence on the Hermitian term of $\mathcal{H}$.

Let us now prove that the equation of motion for the metric $G(t)$ preserves its symmetry, as long as the real and imaginary parts of the Hamiltonian we choose are such that $H(p,q), \Gamma(p,q) \in C^2(\mathbb{R}^2, \mathbb{R})$. With this, we see that both the Hessian matrix of the real part of the Hamiltonian as well as the one of the imaginary part are symmetric. This follows directly from Schwarz's theorem. Furthermore, we know that, in the basis (P, Q) the symplectic form Ω is such that $\Omega^T = -\Omega = \Omega^{-1}$ and so if we transpose the second equation in Eq. (3.8), where we define that $\dot{G}(t) = f(G(t))$, we obtain:

$$\begin{aligned}
\dot{G}^T(t) &= \left(H''(Y)\Omega G - G\Omega H''(Y) + \Gamma''(Y) - G\Gamma''_\Omega(Y)G\right)^T = f(G(t))^T \\
&= (G^T\Omega^T H''(Y)^T - H''(Y)^T\Omega^T G^T + \Gamma''(Y)^T - G^T\Omega^T\Gamma''(Y)^T\Omega G^T) = . \\
&= H''(Y)\Omega G^T - G^T\Omega H''(Y) + \Gamma''(Y) - G^T\Gamma''_\Omega(Y)G^T = f(G^T(t))
\end{aligned} \tag{3.9}$$

An informal argument for assuming that the symmetry of $G(t)$ is preserved is now presented. From the above equation, we see that if we start with an initial symmetric $G_0^T = G_0$ then we have that, for an infinitesimal dt:

$$G(dt) \approx G(0) + dt f(G(0)) = G(0)^T + dt f(G(0)^T) \approx G(dt)^T \ , \tag{3.10}$$

meaning that we will always evolve to a matrix that is also symmetric. Doing these dt steps infinitely many times would lead us to conclude that $G(t)^T = G(t)$.

3.3 Solving the system of equations

3.3.1 The direct method

The simplest method of solving the system of equations is to try to solve directly the equations for the motion of the center and the metric of the state. This is not always straightforward because both of these equations are coupled to each other, meaning that there is a dependence on a given equation of the solutions for the other. This makes the process of analytically solving the system of equations cumbersome barring some special cases.

One class of Hamiltonians for which it is possible to analytically solve the equations is for quadratic Hamiltonians. This is due to the fact that the Hessian matrices for both H and Γ do not depend on the coordinates of the center. Thus, we solve the matrix differential equation and obtain the dynamics for $G(t)$. Afterwards, we substitute $G(t)$ in the equation for the center and solve it to obtain the motion of the center, $Y(t)$. Lastly, we use both $Y(t)$ and $G(t)$ to obtain the dynamics of the coefficient $\alpha(t)$, that multiplies the exponential factor in Eq. (2.14).

3.3.2 Alternative method of decoupling the equations for the center from the equations for the intrinsic geometry of the state

Another option, is to make use of the Kähler structure underlying the system, in particular Eq. (2.9) in order to write the following:

$$G = \Omega J \Leftrightarrow G^{-1}GJ = G^{-1}\Omega J^2 \Leftrightarrow J = -G^{-1}\Omega \Leftrightarrow J\Omega = G^{-1} \ . \tag{3.11}$$

With the above, we can rewrite the equation for the evolution of the center into Eq. (2.18).

It follows from [24, 29] that a solution to the coupled system of equations for the center and the intrinsic geometry of the Gaussian coherent states can be found as follows: First, we calculate the flow in $\mathbb{C}^2$ of the complex vector field $-X_{\mathcal{H}} : (p_t, q_t)$. Then, we find the unique, if it exists, diffeomorphism $\tilde{\varphi}_t^{-X_{\mathcal{H}}} : \mathbb{R}^2 \to \mathbb{R}^2$ such that:

$$\left(\tilde{\varphi}_t^{-X_{\mathcal{H}}}\right)^* (z_0(p,q)) = e^{-tX_{\mathcal{H}}} z_0(p,q) = z_t(p,q) = z_0(p_t, q_t) \ , \tag{3.12}$$

where z_0 denotes the global complex coordinate defining J_0. After that, the solution of Eqs. (2.17) is given by $\varphi_t = \left(\tilde{\varphi}_t^{-X_{\mathcal{H}}}\right)^{-1}$, i.e.:

$$Y_t = \varphi_t^* (Y_0) \tag{3.13}$$

$$G_t = \Omega \left(\varphi_t^{-1}\right)^* (J_0) \ . \tag{3.14}$$

The intuition behind this method is that, we evolve the state using the complex vector field $-X_{\mathcal{H}}$. However, for the centers of the state, the opposite is true i.e., they should evolve not with $-X_{\mathcal{H}}$ but in the opposite direction of the evolution of the state, which corresponds to $X_{\mathcal{H}}$, as seen in Eq. (2.19).

We remark that, for real Hamiltonians we have:

$$\left(\varphi_t^{-X_{\mathcal{H}}}\right)^{-1} = \varphi_t^{X_{\mathcal{H}}} \,, \tag{3.15}$$

however, for complex Hamiltonians the same cannot be said. Arguments from geometric quantization [24, 29] seem to indicate that, for non quadratic Hamiltonians, the equations for the motion of the center as described by this methodology might give a better approximation than the ones described in Eqs. (3.8).

3.3.3 From holomorphic coordinates to J and G

To apply this method we need to choose an appropriate complex coordinate such that we reobtain the initial complex structure and, consequently, the initial metric. We know that, if we were to choose the complex $J-$holomorphic coordinate $z = x + iy$ then, in the (x, y) basis, the complex structure is:

$$J = \begin{pmatrix} 0 & -1 \\ 1 & 0 \end{pmatrix} \,. \tag{3.16}$$

The method to calculate J is by noticing that, from the definition of z and $\bar{z}$, we have:

$$\begin{cases} dz = dx + idy \\ d\bar{z} = dx - idy \end{cases} \Leftrightarrow \begin{pmatrix} dz \\ d\bar{z} \end{pmatrix} = M \begin{pmatrix} dx \\ dy \end{pmatrix} \,, \tag{3.17}$$

where M is the matrix encapsulating the transformation from $dz, d\bar{z}$ to dx, dy. And so, using Eq. (2.4), we can rewrite the definition of J:

$$J = i\frac{\partial}{\partial z} \otimes dz - i\frac{\partial}{\partial \bar{z}} \otimes d\bar{z} \,, \tag{3.18}$$

to obtain the standard complex structure.

However let us now analyze the case where we have $z = x + (a + ib)y$, or another linear transformation of coordinates. In that case we have:

$$\begin{cases} dz = (b + ia)dx + idy \\ d\bar{z} = (b - ia)dx - idy \end{cases} \Leftrightarrow \begin{pmatrix} dz \\ d\bar{z} \end{pmatrix} = M \begin{pmatrix} dx \\ dy \end{pmatrix} \Leftrightarrow \begin{pmatrix} dx \\ dy \end{pmatrix} = M^{-1} \begin{pmatrix} dz \\ d\bar{z} \end{pmatrix} \,, \tag{3.19}$$

like before. However, in order to obtain the expressions for $\partial_z, \partial_{\bar{z}}$ we need to consider a test function, $F(x, y) = U(x, y) + iV(x, y)$. The differential of this test function is given by:

$$dF = \frac{\partial F}{\partial x}dx + \frac{\partial F}{\partial y}dy = dz\left(M_{11}^{-1}\frac{\partial F}{\partial x} + M_{21}^{-1}\frac{\partial F}{\partial y}\right) + d\bar{z}\left(M_{12}^{-1}\frac{\partial F}{\partial x} + M_{22}^{-1}\frac{\partial F}{\partial y}\right) := \frac{\partial F}{\partial z}dz + \frac{\partial F}{\partial \bar{z}}d\bar{z} \,, \tag{3.20}$$

and so we have that:

$$\begin{pmatrix} \partial_z \\ \partial_{\bar{z}} \end{pmatrix} = \left(M^{-1}\right)^T \begin{pmatrix} \partial_x \\ \partial_y \end{pmatrix} \,. \tag{3.21}$$

Using the above we can now, for example, see how J is written in the basis (p, q) when we have the complex coordinate $z = p + (-a - ib)q$. Substituting Eq. (3.19) and Eq. (3.21) into Eq. (3.18) thus

gives:

$$J = \begin{pmatrix} -\frac{a}{b} & \frac{a^2+b^2}{b} \\ -\frac{1}{b} & \frac{a}{b} \end{pmatrix} \implies G = \begin{pmatrix} \frac{1}{b} & -\frac{a}{b} \\ -\frac{a}{b} & b + \frac{a^2}{b} \end{pmatrix} , \tag{3.22}$$

where in the last step we used Eq. (2.15). Notice that we obtain precisely the form for the metric matrix as in Eq. (2.9). With this calculation we are able to pass from a given complex structure to its corresponding complex coordinate and vice-versa:

$$z = p + (-a - ib)q \Leftrightarrow G = \begin{pmatrix} \frac{1}{b} & -\frac{a}{b} \\ -\frac{a}{b} & b + \frac{a^2}{b} \end{pmatrix}, \text{ in the basis } (p, q) \tag{3.23}$$

We remark that scaling the entire complex coordinate by a real factor does not affect the resulting metric nor the complex structure. Moreover, a global scale by a complex number also does not change the inherent complex structure. This in turn means that we can either start with a complex coordinate of the form $z = p + (-a - ib)q$ or with $w = -\frac{1}{a+ib}p + q$ as they correspond to the same metric and complex structure. This remark may be helpful in certain examples where a given choice of initial complex coordinate might simplify the process of obtaining the solution.

3.4 Examples

In order to fully understand how the alternative method compares to the usual one, in this section we proceed to apply both of the methods previously mentioned on some examples. Specifically, we discuss both the regular and the imaginary free particle and the harmonic oscillator in imaginary time.

3.4.1 Free particle in imaginary time

In this example we consider a free particle evolving in imaginary time, i.e., we consider the following Hamiltonian:

$$\mathcal{H} = -\frac{i}{2}p^2 \implies \Gamma = \frac{p^2}{2} , \tag{3.24}$$

with corresponding gradient and hessian:

$$\nabla\Gamma = (p, 0) \qquad \Gamma'' = \begin{pmatrix} 1 & 0 \\ 0 & 0 \end{pmatrix} \tag{3.25}$$

This specific Hamiltonian is interesting to study because we have a way of solving the dynamics of the evolution of the state that is not based on Eq. (3.8) and, through it, we can make an observation regarding the imaginary time evolution of states.

3.4.1.A Explicit method of solving the Schrödinger equation

The method that works for this specific case makes use of fact that we can derive explicitly how the operator $e^{t\frac{\partial^2}{\partial x^2}}$ acts on a function $f(x)$.

In fact, consider the quantum operator version of the Hamiltonian, $\mathcal{H}$:

$$\hat{\mathcal{H}} = -\frac{i}{2}\hat{p}^2 \ . \tag{3.26}$$

Then, by the Schrödinger equation, we have that a wave function $\psi_0(x)$ evolves in the following form:

$$\psi_t(x) = \exp\left[-\frac{i}{\hbar}\hat{H}t\right]\psi_0(x) = \exp\left[i\frac{\hbar t}{2}\frac{\partial^2}{\partial x^2}\right]\psi_0(x) = \exp\left[it'\frac{\partial^2}{\partial x^2}\right]\psi_0(x), \tag{3.27}$$

with $t' = t\hbar/2$.

The system is initially in a Gaussian state of the form of Eq. (2.10). In appendix A we show how the operator $e^{t'\frac{\partial^2}{\partial x^2}}$ acts on a function $f(x)$, yielding:

$$\psi_{t'}(x) = e^{t'\frac{\partial^2}{\partial x^2}}\psi_0(x) = \int_{-\infty}^{\infty} dy\psi_0(y)\left(\frac{1}{4\pi t'}\right)^{\frac{1}{2}} e^{-(x-y)^2/4t'} \tag{3.28}$$

In order to make the calculations clearer we assume that the state is centered at the origin and that the parameter $B = ib$. Thus we have:

$$\psi_0(x) = \left(\frac{b}{\pi\hbar}\right)^{\frac{1}{4}} e^{-\frac{bx^2}{2\hbar}} \ , \tag{3.29}$$

and as the integral is of a Gaussian function it is solvable, giving the following form for $\psi_t(x)$:

$$\psi_t(x) = \left(\frac{b}{\pi\hbar}\right)^{\frac{1}{4}}\left(\frac{\hbar}{2bt'+\hbar}\right)^{\frac{1}{2}}\exp\left[-\frac{x^2}{2}\left(\frac{b}{2bt'+\hbar}\right)\right] = \left(\frac{b}{\pi\hbar}\right)^{\frac{1}{4}}\left(\frac{1}{bt+1}\right)^{\frac{1}{2}}\exp\left[-\frac{1}{\hbar}\frac{x^2}{2}\left(\frac{b}{bt+1}\right)\right] \ , \tag{3.30}$$

where in the end we resubstituted $t' = \hbar t/2$. Note that this state is no longer normalized for positive t, with the norm going to zero as $t \to \infty$. Moreover, note that $b \to \frac{b}{1+bt}$ which gives rise to the metric:

$$G(t) = \begin{pmatrix} t + \frac{1}{b} & 0 \\ 0 & \frac{b}{bt+1} \end{pmatrix} \ . \tag{3.31}$$

This example is interesting because, through it, we can see that the imaginary time evolution of quantum states is analogous to having that state evolve as if were a solution to the heat equation. In particular, $t \to it$ for the free particle makes it so that increasing t leads to the spreading of the localized state across the phase space.

However, for more complicated Hamiltonians this connection is more complicated to discern as we have contributions from real time evolution as well as imaginary time evolution.

3.4.1.B Direct method of solving the system of equations for the center and geometry

Under this Hamiltonian we have the following simplified system of equations:

$$\begin{aligned} \dot{Y} &= -G^{-1}\nabla\Gamma(Y) \\ \dot{G} &= \Gamma''(Y) - G\Gamma''_\Omega(Y)G \\ \frac{\dot{\alpha}}{\alpha} &= -\frac{2}{\hbar}\Gamma(Y) - \frac{1}{2}\operatorname{Tr}\left[\Gamma''_\Omega(Y)G\right] \end{aligned} \ , \tag{3.32}$$

which we now proceed to solve.

We start by solving the metric equation. If we assume that G is of the form:

$$G(t) = \begin{pmatrix} g_1(t) & g_3(t) \\ g_3(t) & g_2(t) \end{pmatrix} , \tag{3.33}$$

then the equation for its time derivative is:

$$\dot{G}(t) = \begin{pmatrix} 1 - g_3(t)^2 & -g_2(t)g_3(t) \\ -g_2(t)g_3(t) & -g_2(t)^2 \end{pmatrix} . \tag{3.34}$$

We start by solving the equation for $g_2(t)$. It is a separable equation with solution:

$$g_2(t) = \frac{g_2(0)}{1 + g_2(0)t} . \tag{3.35}$$

From this solution we can also obtain the solution to the equation for $g_3(t)$, as it is also separable, and we get:

$$g_3(t) = \frac{g_3(0)}{1 + g_2(0)t} . \tag{3.36}$$

Lastly we can obtain the solution for $g_1(t)$ from the last one by solving another separable differential equation:

$$g_1(t) = \frac{g_1(0) + t + \left(g_1(0)g_2(0) - g_3(0)^2\right) t + g_2(0)t^2}{1 + g_2(0)t} = \frac{g_1(0) + 2t + g_2(0)t^2}{1 + g_2(0)t} , \tag{3.37}$$

where in the last step we used the fact that the initial metric matrix had $\det G(0) = 1$.

Rounding all solutions together we obtain:

$$G(t) = \frac{1}{1 + g_2(0)t} \begin{pmatrix} g_1(0) + 2t + g_2(0)t^2 & g_3(0) \\ g_3(0) & g_2(0) \end{pmatrix} . \tag{3.38}$$

We can check that this matrix has $\det G(t) = 1, \forall t \in \mathbb{R}_0^+$. In fact, in this case, because we can see see that the determinant of the metric is invariant, we could obtain any one of the components if we knew the other two.

The inverse of the metric matrix is:

$$G(t)^{-1} = \frac{1}{1 + g_2(0)t} \begin{pmatrix} g_2(0) & -g_3(0) \\ -g_3(0) & g_1(0) + 2t + g_2(0)t^2 \end{pmatrix} , \tag{3.39}$$

and, with the above, we now solve the equation for the motion of the center:

$$\begin{pmatrix} \dot{P}(t) \\ \dot{Q}(t) \end{pmatrix} = \frac{1}{1 + g_2(0)t} \begin{pmatrix} -g_2(0)P(t) \\ g_3(0)P(t) \end{pmatrix} , \tag{3.40}$$

whose solution is:

$$\begin{cases} P(t) = \frac{P(0)}{1+g_2(0)t} \\ Q(t) = Q(0) + \frac{P(0)g_3(0)t}{1+g_2(0)t} \end{cases} . \tag{3.41}$$

At $t = 0$ we have $Y(0) = (P(0), Q(0))$ and when $t \to +\infty$ we have, by taking the limit of Eq. (3.41),

that $Y(t \to +\infty) = (0, Q(0) + \frac{P(0)g_3(0)}{g_2(0)})$.

By making a change of variables, it is possible to show that the position coordinate of the center depends solely on the momentum one, i.e., we can show that:

$$Q(P(t)) = Q(0) + \frac{g_3(0)}{g_2(0)} - \frac{g_3(0)}{g_2(0)} P(t) \ , \tag{3.42}$$

where the values for the constants are taken when $t = 0$. Thus, we have shown that the trajectory in phase space for the motion of the center is a line segment with slope equal to $\frac{g_3(0)}{g_2(0)}$. Using Eq. (3.1) we can see that the slope, in terms of the parameter $B = re^{i\theta}$ of the initial Gaussian state, is given by $-\frac{\cos\theta}{r}$. Given the fact that the parameter B lies on the upper half complex plane this implies that all slope values are possible under this Hamiltonian.

As an example, in Fig. (3.4) we can see the trajectory across time for a state with initial center $Y(0) = (3, 2)$ and initial metric $G = \begin{pmatrix} 1 & -1 \\ -1 & 2 \end{pmatrix}$.

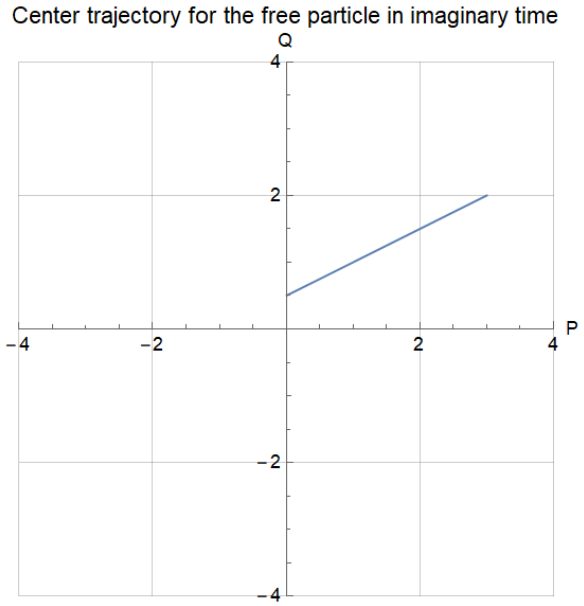

Figure 3.4: Time trajectory for the center of a state with initial center $Y(0) = (3, 2)$ and initial metric induced by the parameter $B = 1 + i$, when evolved using the Hamiltonian in Eq. (3.24)

As predicted by Eq. (3.41), we expect the center to move towards the point $Y(t \to \infty) = (0, Q(0) + \frac{P(0)g_3(0)}{g_2(0)}) = (0, \frac{1}{2})$ as $t \to \infty$. We can confirm that in the above figure. Furthermore we also can see that the trajectory follows a line segment with the predicted slope.

Lastly, to conclude this example we just need to solve the equation for the parameter $\alpha(t)$, which begins at one, as the initial state is always considered to be normalized. So, substituting the solutions above in the third equation in Eq. (3.32) and solving it, yields:

$$\alpha(t) = \frac{\exp\left[-\frac{P(0)^2 t}{\hbar(1+g_2(0)t)}\right]}{\sqrt{g_2(0)t + 1}} \ , \tag{3.43}$$

which is an exponentially decreasing function. We can interpret this loss of "probability" as some sort

of loss of energy of the system to the environment.

3.4.1.C Alternative method of solving the system of equations for the center and geometry

Having solved this in two other ways, let us now put in practice the alternative method. The complex vector field $-X_{\mathcal{H}}$, in this example reads:

$$-X_{\mathcal{H}} = ip\frac{\partial}{\partial q} \ . \tag{3.44}$$

Choosing a general initial complex structure or metric amounts to, as discussed in subsection 3.3.3, choosing the following initial complex coordinate:

$$z_0 = p - (a+ib)q \ , \tag{3.45}$$

where we see that:

$$\begin{cases} q = -\frac{1}{b}\,\mathrm{Im}(z) \\ p = \mathrm{Re}(z) - \frac{a}{b}\,\mathrm{Im}(z) \end{cases} \tag{3.46}$$

Furthermore, let us now apply the Hamiltonian complex flow to our holomorphic coordinate:

$$z_t = e^{-tX_{\mathcal{H}}} z_0 = e^{itp\frac{\partial}{\partial q}}(p + (a+ib)q) = p - (a+ib)(q+itp) =: p_t - (a+ib)q_t \ . \tag{3.47}$$

In order to find, p_t, q_t we use Eqs. (3.46) which yield:

$$\begin{cases} q_t = q + \frac{a}{b}pt \\ p_t = p(1 + \frac{a^2+b^2}{b}t) \end{cases} \Leftrightarrow \begin{pmatrix} p_t \\ q_t \end{pmatrix} = \begin{pmatrix} 1 + (\frac{a^2}{b} + b)t & 0 \\ \frac{a}{b}t & 1 \end{pmatrix} \begin{pmatrix} p \\ q \end{pmatrix} \ , \tag{3.48}$$

where we now must invert the above matrix to get φ_t:

$$\varphi_t = \begin{pmatrix} \frac{1}{1+\left(\frac{a^2}{b}+b\right)t} & 0 \\ -\frac{\frac{a}{b}t}{1+\left(\frac{a^2}{b}+b\right)t} & 1 \end{pmatrix} \ . \tag{3.49}$$

Finally, from the above we can directly obtain:

$$Y_t = \begin{pmatrix} P(t) \\ Q(t) \end{pmatrix} = \varphi_t^*(Y_0) = \begin{pmatrix} \frac{P(0)}{1+\left(\frac{a^2}{b}+b\right)t} \\ Q(0) - \frac{\frac{a}{b}P(0)t}{1+\left(\frac{a^2}{b}+b\right)t} \end{pmatrix} \ , \tag{3.50}$$

which is exactly the same motion for the center as the one obtained in Eqs. (3.41), noticing that $g_2(0) = \frac{a^2}{b} + b$ and $g_3(0) = -\frac{a}{b}$.

Now, for the complex structure J_t we note that we had, in Eq. (3.47), that:

$$z_t = p(1 + bt - iat) + q(-a - ib) \ . \tag{3.51}$$

Now, following the process described in subsection 3.3.3, we can find the complex structure associ-

ated with z_t and obtain G_t from it. Doing this process, yields:

$$G(t) = \begin{pmatrix} \frac{t^2\left(a^2+b^2\right)+2bt+1}{t(a^2+b^2)+b} & -\frac{a}{t(a^2+b^2)+b} \\ -\frac{a}{t(a^2+b^2)+b} & \frac{a^2+b^2}{t(a^2+b^2)+b} \end{pmatrix} , \tag{3.52}$$

which is precisely the same matrix as in Eq. (3.38). We managed to, algebraically, get both the motion of the real center of the Wigner function and the motion of the intrinsic metric. To do so, we just needed to calculate the complex Hamiltonian vector field and apply it to an initial holomorphic coordinate. From thereon, we followed the procedure developed in subsection 3.3.2 to arrive at the same results as the ones obtained through the direct method of solving the entire Eq. (3.8).

3.4.2 Free particle

As a sanity check, let us observe the predicted dynamics for a wave packet under the formalisms previously introduced in the regular free particle. Thus, the Hamiltonian is $\mathcal{H} = \frac{p^2}{2}$.

For a regular wave packet centered at $(P(0), Q(0))$ we expect that, as time increases, the center of the Wigner function moves towards the point $(P(0), Q(0) + tP(0))$. Furthermore, we also expect the position wave function to spread with time.

In Eq. (2.10), when the parameter B is purely imaginary we have the following metric:

$$G = \begin{pmatrix} \frac{1}{b} & 0 \\ 0 & b \end{pmatrix} , \tag{3.53}$$

and thus we can see that if we decrease b this leads to the wave packet being more stretched, when projected to the position basis.

In this specific case the solution of Eq. (3.8) is straightforward. In this case the equations are not coupled due to the fact that $\Gamma = 0$. As such, the equations of motion for the center follow the usual Hamiltonian flow:

$$\begin{cases} \dot{P} = -\frac{\partial H}{\partial Q} = 0 \\ \dot{Q} = \frac{\partial H}{\partial P} = P \end{cases} \implies \begin{cases} P(t) = P(0) \\ Q(t) = Q(0) + P(0)t \end{cases} . \tag{3.54}$$

Meaning that we obtain the expected motion for the center. As for the metric we solve the differential equation for $G(t)$ in the same manner as the example before, obtaining, in the general case:

$$G(t) = \begin{pmatrix} \frac{t^2\left(a^2+b^2\right)+2at+1}{b} & -\frac{t\left(a^2+b^2\right)+a}{b} \\ -\frac{t\left(a^2+b^2\right)+a}{b} & \frac{a^2}{b}+b \end{pmatrix} , \tag{3.55}$$

which in our case as $a = 0$ reduces to:

$$G(t) = \begin{pmatrix} bt^2 + \frac{1}{b} & -tb \\ -tb & b \end{pmatrix} . \tag{3.56}$$

Notice that, from Eq. (3.3), we can see that as time increases the imaginary component of B goes to zero. This in turn means that the position wave function spread is also growing with time. Thus we see that we obtain the predicted behavior under this formalism.

We could also redo the same calculations using the alternative method. Starting with $z_0 = p - ibq$ and $-X_{\mathcal{H}} = -p\frac{\partial}{\partial q}$, we obtain:

$$z_t = p(1 + ibt) - ibq \ , \tag{3.57}$$

whose inherent complex structure leads to the same metric as the one obtained before.

3.4.3 Harmonic oscillator in imaginary time

We now consider an Hamiltonian of the following form:

$$\mathcal{H} = -i\left(\frac{p^2}{2} + \frac{x^2}{2}\right) \ , \tag{3.58}$$

which corresponds to an harmonic oscillator in imaginary time. When calculating the equation for $G(t)$:

$$G(t) = \begin{pmatrix} g_1(t) & g_3(t) \\ g_3(t) & g_2(t) \end{pmatrix} \ , \tag{3.59}$$

using Eq. (3.8), we obtain:

$$\begin{cases} \dot{g_1}(t) = 1 - g_1(t)^2 - g_3(t)^2 \\ \dot{g_2}(t) = 1 - g_2(t)^2 - g_3(t)^2 \\ \dot{g_3}(t) = g_3(t)\left(-g_1(t) - g_2(t)\right) \end{cases} \ , \tag{3.60}$$

which is a system of three non linear ordinary differential equations. We could not figure how to solve this system analytically in the direct case. However, if we assume that $g_3(0) = 0$ then we can solve it.

3.4.3.A Direct method of solving the system of equations for the center and geometry

Let us assume that $G(t)$ is a real analytic function. In that case, the Taylor series for the component $g_3(t)$ around the origin is:

$$g_3(t) = \sum_{n=0}^{+\infty} \frac{g_3^{(n)}(0)}{n!} t^n \ . \tag{3.61}$$

As $G(t)$ is real analytic then $g_1(t), g_2(t)$ as well as their derivatives are well defined and exist. Furthermore, suppose we have $g_3(0) = 0$. By Eq. (3.60) we also know that $\dot{g_3}(0) = 0$. And so, we can differentiate again the equation for $\dot{g}_3(t)$ in Eq. (3.60) to get:

$$\ddot{g_3}(t) = -\dot{g_3}(t)(g_1(t) + g_2(t)) - g_3(t)(\dot{g_1}(t)\dot{g_2}(t) + g_1(t) + g_2(t)) \ , \tag{3.62}$$

which again at $t = 0$ gives $\ddot{g_3}(0) = 0$. In general we see that, if we keep differentiating we will obtain an expression of the form:

$$g_3^{(n)}(t) = \sum_{k=0}^{n-1} g_3^{(k)}(t) F_{n-1-k}(g_1(t), g_2(t)) \ , \tag{3.63}$$

where:

$$F_k(g_1(t), g_2(t)) = \sum_{m=0}^{k} \left(C_m g_1^{(m)}(t) + D_m g_2^{(m)}(t)\right) \quad , C_m, D_m \in \mathbb{R}, \tag{3.64}$$

meaning F_k is made up of sums of terms which depend on, at most, the k derivatives of $g_1(t), g_2(t)$. All of this to argue that, if we set $t = 0$ we can recursively see that all derivatives are zero.

Thus, we are prone to conclude that, if $g_3(0) = 0$ then $g_3(t) = 0$ and thus the equations to solve for the metric reduce to:

$$\begin{cases} \dot{g}_1(t) = 1 - g_1(t)^2 \\ \dot{g}_2(t) = 1 - g_2(t)^2 \end{cases} . \tag{3.65}$$

The above are two decoupled Riccati equations. A Riccati equation is an ordinary differential equation that is quadratic on the unknown function. It suffices to solve the equation for just one of the components of the matrix. To see why we define $f(t) = \frac{1}{g_1(t)}$ and so:

$$\dot{f}(t) = -\frac{1}{g_1(t)^2}\dot{g}_1(t) \Leftrightarrow \dot{g}_1(t) = -\frac{\dot{f}(t)}{f(t)^2} . \tag{3.66}$$

Substituting both $f(t)$ and $\dot{f}(t)$ on the equation for $\dot{g}_1(t)$ gives:

$$-\frac{\dot{f}(t)}{f(t)^2} = 1 - \frac{1}{f(t)} \Leftrightarrow \dot{f}(t) = 1 - f(t)^2 , \tag{3.67}$$

where in the last step we just multiplied the entire equation by $-f(t)^2$. This means that $\frac{1}{g_1(t)}$ also obeys the same equation as $g_1(t)$. Also, because $g_3(t) = 0$ then the parameter $B = a + ib$ has to be purely imaginary, which leads to an initial metric $G(0) = \mathrm{diag}\left(\frac{1}{b}, b\right)$. This means that $g_1(0) = \frac{1}{g_2(0)}$ meaning that the function $f(t)$ that we had defined is in fact $g_2(t)$. We have thus proved that we only need to solve the equation for one of the components of the metric, with the other being henceforth completely determined.

Equation (3.66) is separable and solvable by partial fraction decomposition:

$$\begin{aligned} \frac{df}{1-f^2} &= dt \\ \Leftrightarrow \frac{df}{1+f} + \frac{df}{1-f} &= 2dt \\ \Leftrightarrow \log\left(\frac{1+f}{1-f}\right) &= 2t + C \\ \Leftrightarrow f(t) &= \frac{Ce^t - e^{-t}}{Ce^t + e^{-t}} , \end{aligned} \tag{3.68}$$

and, when we substitute C for the initial condition of $f(t)$ we get:

$$f(t) = \frac{f(0)\cosh(t) + \sinh(t)}{\cosh(t) + f(0)\sinh(t)} . \tag{3.69}$$

If, $f(t) = g_1(t)$ then $f(0) = \frac{1}{b}$ and we get:

$$g_1(t) = \frac{b\sinh(t) + \cosh(t)}{b\cosh(t) + \sinh(t)} , \tag{3.70}$$

which gives the metric:

$$G(t) = \begin{pmatrix} \frac{b\sinh(t)+\cosh(t)}{b\cosh(t)+\sinh(t)} & 0 \\ 0 & \frac{b\cosh(t)+\sinh(t)}{b\sinh(t)+\cosh(t)} \end{pmatrix} . \tag{3.71}$$

Substituting this onto the equation for the center in Eq. (3.8) and solving it yields:

$$\begin{cases} P(t) = \frac{P(0)}{b\sinh(t)+\cosh(t)} \\ Q(t) = \frac{bQ(0)}{b\cosh(t)+\sinh(t)} \end{cases}, \tag{3.72}$$

which is a motion that, as $t \to +\infty$, tends to the origin no matter the initial conditions.

Finally, we solve the equation for the factor $\alpha(t)$ to obtain:

$$\alpha(t) = \frac{\sqrt{2b}\exp\left(-\sinh(t)\left(\frac{P(0)^2}{b\sinh(t)+\cosh(t)} + \frac{bQ(0)^2}{b\cosh(t)+\sinh(t)}\right)\right)}{\sqrt{(b^2+1)\sinh(2t)+2b\cosh(2t)}} \tag{3.73}$$

As a specific example, we take an initial Wigner function, given by Eq. (2.14), with $G = \mathrm{diag}(1/2, 2)$ and $(P, Q) = (2, 0)$. Under the harmonic oscillator in imaginary time, the evolution for the center is:

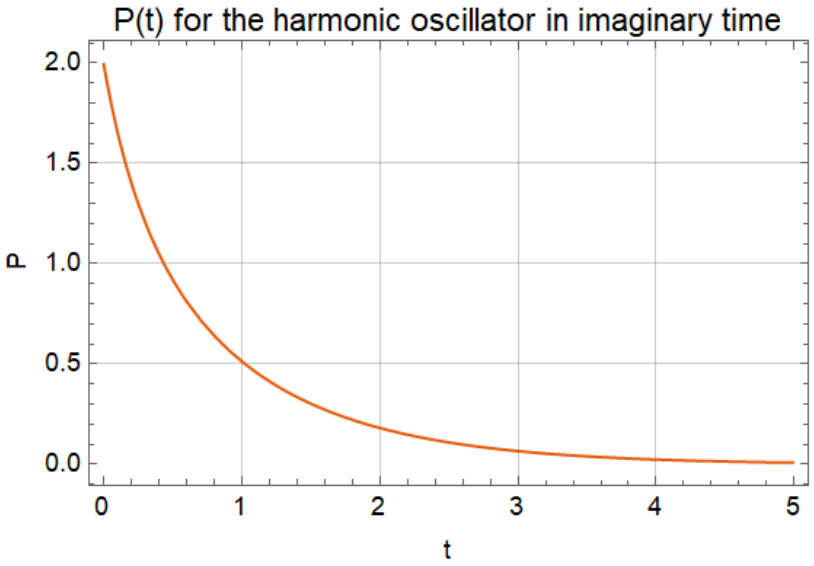

Figure 3.5: Plot for the motion with time of the momentum component of the center of a coherent Wigner function (Eq. (2.14)) with time. The initial function has initial metric $G = \mathrm{diag}(1/2, 2)$ and center $(P, Q) = (2, 0)$.

where we did not plot the position component as it remains at its initial position. Moreover, the solution for the metric with time is:

$$G(t) = \begin{pmatrix} \frac{2\sinh(t)+\cosh(t)}{\sinh(t)+2\cosh(t)} & 0 \\ 0 & \frac{\sinh(t)+2\cosh(t)}{2\sinh(t)+\cosh(t)} \end{pmatrix}, \tag{3.74}$$

where we can see that, for large t it is approaching the identity matrix.

In fact, no matter the initial conditions for the center or metric we always observe the same behavior. The center moves towards the origin whereas the metric tends towards the identity matrix. Thus, this system always tends towards the coherent Wigner function at the origin, with no squeezing present. The only difference is that the factor $\alpha(t)$ is tending towards zero as time increases.

The above general motion follows directly from the fact that both $\sinh(t), \cosh(t)$ approach $e^t/2$ as time increases. However, Eq. (3.71) was only derived assuming an initial metric. To obtain a generic expression for an arbitrary initial parameter, $B = a + ib,\ b > 0$ we must turn to the alternative method.

Doing so will allow us to confirm the claim that the metric will always approach the identity matrix for large enough time.

3.4.3.B Alternative method of decoupling the systems of equations for the center and the geometry

We will now apply the alternative method to a general choice of initial metric. The complex vector field $-X_{\mathcal{H}}$, in this example reads:

$$-X_{\mathcal{H}} = ip\frac{\partial}{\partial q} - iq\frac{\partial}{\partial q} \ . \tag{3.75}$$

Like before, choosing a general initial complex structure or metric amounts to choosing the following initial complex coordinate:

$$z_0 = p - (a+ib)q \ . \tag{3.76}$$

We now want to apply the Hamiltonian complex flow to our holomorphic coordinate. To do that, however, we first note that:

$$\dot{p}_t = \frac{\partial}{\partial t}\left(e^{-X_{\mathcal{H}}t}p\right) = e^{-X_{\mathcal{H}}t}\left(-X_{\mathcal{H}}p\right) = -iq_t \tag{3.77}$$

$$\dot{q}_t = \frac{\partial}{\partial t}\left(e^{-X_{\mathcal{H}}t}q\right) = e^{-X_{\mathcal{H}}t}\left(-X_{\mathcal{H}}q\right) = ip_t \ . \tag{3.78}$$

To solve the above system we differentiate $\dot{p}_t$ to get:

$$\ddot{p}_t = -i\dot{q}_t = p_t \ , \tag{3.79}$$

whose general solution is given by a linear combination of two exponentials, e^t, e^{-t} or, equivalently by a linear combination of $\cosh(t), \sinh(t)$. We take $p_t = A\cosh(t) + B\sinh(t)$ and substitute in the equation for $\dot{q}_t$ to get:

$$\dot{q}_t = iA\cosh(t) + iB\sinh t \implies q_t = iA\sinh(t) + iB\cosh(t) + C \ . \tag{3.80}$$

Now we know from the initial conditions that:

$$\begin{cases} p_0 = p = A \\ q_0 = q = C + iB \\ \dot{p}_0 = B \\ -iq_0 = B \end{cases} \Leftrightarrow \begin{cases} A = p \\ B = -iq \\ C = 0 \end{cases} \ . \tag{3.81}$$

The motion of the complexified center is thus:

$$\begin{cases} p_t = p\cosh(t) - iq\sinh(t) \\ q_t = q\cosh(t) + ip\sinh(t) \end{cases} \ , \tag{3.82}$$

which we proceed to use to obtain:

$$z_t = e^{-tX_{\mathcal{H}}}z_0 = \left(p\cosh(t) - iq\sinh(t)\right) - (a+ib)\left(q\cosh(t) + ip\sinh(t)\right) \ . \tag{3.83}$$

In order to find, p_t, q_t as defined in $z_0 = p_t - (a+ib)q_t$, we again make use of Eqs. (3.46) which yield:

$$\begin{pmatrix} p_t \\ q_t \end{pmatrix} = \begin{pmatrix} \cosh t + \left(\frac{a^2}{b} + b\right)\sinh t & \frac{a}{b}\sinh t \\ \frac{a}{b}\sinh t & \cosh t + \frac{1}{b}\sinh t \end{pmatrix} \begin{pmatrix} p \\ q \end{pmatrix} , \tag{3.84}$$

where we, before inverting the above matrix, substitute the initial conditions for the metric to get:

$$\begin{pmatrix} p_t \\ q_t \end{pmatrix} = \begin{pmatrix} \cosh t + g_2(0)\sinh t & -g_3(0)\sinh t \\ -g_3(0)\sinh t & \cosh t + g_1(0)\sinh t \end{pmatrix} \begin{pmatrix} p \\ q \end{pmatrix} , \tag{3.85}$$

where we now invert the above matrix to get φ_t:

$$\varphi_t = \frac{1}{\cosh^2 t + \sinh^2 t + (g_1(0)+g_2(0))\sinh t\cosh t} \begin{pmatrix} \cosh t + g_1(0)\sinh t & g_3(0)\sinh t \\ g_3(0)\sinh t & \cosh t + g_2(0)\sinh t \end{pmatrix} . \tag{3.86}$$

Finally, from the above we can directly obtain:

$$Y_t = \begin{pmatrix} P(t) \\ Q(t) \end{pmatrix} = \varphi_t^*(Y_0) , \tag{3.87}$$

which becomes:

$$\begin{pmatrix} P(t) \\ Q(t) \end{pmatrix} = \frac{1}{\cosh^2 t + \sinh^2 t + (g_1(0)+g_2(0))\sinh t\cosh t} \begin{pmatrix} \cosh t + g_1(0)\sinh t & g_3(0)\sinh t \\ g_3(0)\sinh t & \cosh t + g_2(0)\sinh t \end{pmatrix} \begin{pmatrix} P(0) \\ Q(0) \end{pmatrix} \tag{3.88}$$

from which one can check that, if we set $g_3(0) = 0$ we obtain the same motion for the center as in Eq. (3.72).

Finally, for the complex structure J_t we note that we had, in Eq. (3.83), that:

$$z_t = p(\cosh t + b\sinh t - ia\sinh t) + q(-a\cosh t - ib\cosh t - i\sinh t) . \tag{3.89}$$

Now, following the process described in subsection 3.3.3, we can find the complex structure associated with z_t and obtain G_t from it. Doing this process, yields:

$$G(t) = \begin{pmatrix} \frac{\left(a^2+b^2\right)\sinh^2(t)+b\sinh(2t)+\cosh^2(t)}{\left(a^2+b^2+1\right)\sinh(t)\cosh(t)+b\cosh(2t)} & -\frac{a}{\left(a^2+b^2+1\right)\sinh(t)\cosh(t)+b\cosh(2t)} \\ -\frac{a}{\left(a^2+b^2+1\right)\sinh(t)\cosh(t)+b\cosh(2t)} & \frac{\left(a^2+b^2\right)\cosh^2(t)+b\sinh(2t)+\sinh^2(t)}{\left(a^2+b^2+1\right)\sinh(t)\cosh(t)+b\cosh(2t)} \end{pmatrix} . \tag{3.90}$$

Using this method not only are we able to reobtain the same metric as calculated previously, we also confirm that indeed if $g_3(0) = 0$ then $g_3(t) = 0$. Furthermore, we were also able to get the general expression for the time evolution of $G(t)$. I was not able to obtain Eq. (3.90) using the direct method, not even with the help of the software *Mathematica*. We remark that numerical solutions for Eqs. 3.8 were obtained in order to confirm that the dynamics that were calculated through this method correspond to the dynamics of Eq. (3.8).

This example illustrates the usefulness of the alternative method in facilitating the process of solving the dynamics of both $G(t)$ and $Y(t)$ analytically. We simply need to solve the complex dynamics for the center, which no longer is coupled to $G(t)$. Finally, we can then extract the inherent complex structure from the complex coordinate as well as the real center of the Wigner function. We are able

to turn a problem which involves solving a coupled system of five differential equations into one of solving a coupled system of two differential equations, followed by algebraical manipulations.

3.5 Time evolution of the Wigner function

In this section we derive the equation for the time evolution of the Wigner function under a non-Hermitian Hamiltonian. We start by taking the partial derivative of Eq. (2.11) with respect to time:

$$\frac{\partial W(x,p)}{\partial t} = \int_{-\infty}^{+\infty} \frac{1}{\pi\hbar} \left[\frac{\partial \psi^*(x+y)}{\partial t} \psi(x-y) + \psi^*(x+y) \frac{\partial \psi(x-y)}{\partial t} \right] e^{2ipy/\hbar} dy \ . \tag{3.91}$$

Now, we substitute the partial time derivatives for both the wave function and its complex conjugate using Schrödinger's Equation. We notice that, as we are dealing with non-Hermitian Hamiltonians we must take caution when calculating the complex conjugate of the Schrödinger's equation. For $\hat{\mathcal{H}} = \hat{H} - i\hat{\Gamma}$, where both $\hat{H}, \hat{\Gamma}$ are Hermitian, we have:

$$\begin{aligned} \frac{\partial \psi(x,t)}{\partial t} &= -\frac{i}{\hbar}\hat{\mathcal{H}}\psi(x,t) = -\frac{i}{\hbar}\left(\hat{H} - i\hat{\Gamma}\right)\psi(x,t) \\ \frac{\partial \psi^*(x,t)}{\partial t} &= \frac{i}{\hbar}\hat{\mathcal{H}}^\dagger\psi^*(x,t) = \frac{i}{\hbar}\left(\hat{H} + i\hat{\Gamma}\right)\psi^*(x,t) \end{aligned} \ . \tag{3.92}$$

Using the previous equations on Eq. (3.91) and joining terms we get:

$$\begin{aligned} \frac{\partial W(x,p)}{\partial t} =& \frac{i}{\pi\hbar^2} \int_{-\infty}^{+\infty} \Big[\left(\hat{H}\psi^*(x+y)\right)\psi(x-y) - \psi^*(x+y)\left(\hat{H}\psi(x-y)\right) + \\ &+ \left(i\hat{\Gamma}\psi^*(x+y)\right)\psi(x-y) + \psi^*(x+y)\left(i\hat{\Gamma}\psi(x-y)\right)\Big] e^{2ipy/\hbar} dy \ , \end{aligned} \tag{3.93}$$

which describes exactly the time evolution for the Wigner function.

Due to the linearity of the integral we can construct a generic expression for the time derivative of $W(x,p)$ by studying specific examples of both $\hat{H}$ and $\hat{\Gamma}$. Then, we can sum the contribution of each term for the total partial time derivative. On the remainder of this section we show the resulting equation for some choices of real and imaginary part for the Hamiltonian $\hat{\mathcal{H}}$. One can confirm the derivation for an Hermitian Hamiltonian on [5].

3.5.1 Hamiltonian dependent on position operators

In this section, we adopt the methodology used in [5] for the Hermitian case and extend it to be able to compute both Hermitian and non-Hermitian functions of the position operator.

For the Hermitian case, assume that $\hat{H} = V(\hat{x})$. Then, by Eq. (3.93) we have:

$$\frac{\partial W(x,p)}{\partial t} = \frac{i}{\pi\hbar^2} \int_{-\infty}^{\infty} dy e^{2ipy/\hbar} \left(V(x+y) - V(x-y)\right) \psi^*(x+y)\psi(x-y) \ . \tag{3.94}$$

Writing the Taylor series of the potential function around the point x we get that:

$$V(x+y) - V(x-y) = \sum_{n=0}^{+\infty} \frac{1}{n!} \frac{\partial^n V(x)}{\partial x^n} \left(1 - (-1)^n\right) y^n = \sum_{s=0}^{+\infty} \frac{2}{(2s+1)!} \frac{\partial^{2s+1} V(x)}{\partial x^{2s+1}} y^{2s+1} \ , \tag{3.95}$$

which when substituted in the previous equation yields:

$$\frac{\partial W(x,p)}{\partial t} = \sum_{s=0}^{+\infty} \frac{2i}{\pi\hbar^2} \frac{1}{(2s+1)!} \frac{\partial^{2s+1} V(x)}{\partial x^{2s+1}} \int_{-\infty}^{\infty} dy y^{2s+1} e^{2ipy/\hbar} \psi^*(x+y)\psi(x-y) = \tag{3.96}$$

$$= \sum_{s=0}^{+\infty} \frac{2i}{\pi\hbar^2} \frac{1}{(2s+1)!} \frac{\partial^{2s+1} V(x)}{\partial x^{2s+1}} \left(\frac{\hbar}{2i}\frac{\partial}{\partial p}\right)^{2s+1} \int_{-\infty}^{\infty} dy e^{2ipy/\hbar} \psi^*(x+y)\psi(x-y) = \tag{3.97}$$

$$= \sum_{s=0}^{+\infty} \frac{1}{(2s+1)!} \frac{1}{2^{2s}} (-\hbar^2)^s \frac{\partial^{2s+1} V(x)}{\partial x^{2s+1}} \frac{\partial^{2s+1} W(x,p)}{\partial p^{2s+1}} \ . \tag{3.98}$$

As for the non-Hermitian case, with $\hat{\Gamma} = V(\hat{x})$ we would have, by Eq. (3.93):

$$\frac{\partial W(x,p)}{\partial t} = \frac{-1}{\pi\hbar^2} \int_{-\infty}^{\infty} dy e^{2ipy/\hbar} \left(V(x+y) + V(x-y)\right) \psi^*(x+y)\psi(x-y) \ . \tag{3.99}$$

This time, the Taylor series is written as:

$$V(x+y) + V(x-y) = \sum_{n=0}^{+\infty} \frac{1}{n!} \frac{\partial^n V(x)}{\partial x^n} \left(1 + (-1)^n\right) y^n = \sum_{s=0}^{+\infty} \frac{2}{(2s)!} \frac{\partial^{2s} V(x)}{\partial x^{2s}} y^{2s} \ , \tag{3.100}$$

which, when substituted in the previous equation yields:

$$\frac{\partial W(x,p)}{\partial t} = \sum_{s=0}^{+\infty} \frac{-2}{\pi\hbar^2} \frac{1}{(2s)!} \frac{\partial^{2s} V(x)}{\partial x^{2s}} \int_{-\infty}^{\infty} dy y^{2s} e^{2ipy/\hbar} \psi^*(x+y)\psi(x-y) = \tag{3.101}$$

$$= \sum_{s=0}^{+\infty} \frac{-2}{\pi\hbar^2} \frac{1}{(2s)!} \frac{\partial^{2s} V(x)}{\partial x^{2s}} \left(\frac{\hbar}{2i}\frac{\partial}{\partial p}\right)^{2s} \int_{-\infty}^{\infty} dy e^{2ipy/\hbar} \psi^*(x+y)\psi(x-y) = \tag{3.102}$$

$$= \sum_{s=0}^{+\infty} \frac{1}{(2s)!} \frac{1}{2^{2s-1}} (-1)^{s+1} \hbar^{2s-1} \frac{\partial^{2s} V(x)}{\partial x^{2s}} \frac{\partial^{2s} W(x,p)}{\partial p^{2s}} \ . \tag{3.103}$$

3.5.2 Hamiltonian dependent on momentum operators

In this section we consider the case where the Hamiltonian is simply a function of the momentum operator. It is useful to consider another way of writing the Wigner function, which is obtained through the momentum space wave function $\varphi(p)$ (see appendix C):

$$W(x,p) = \frac{1}{\pi\hbar} \int_{-\infty}^{\infty} dy \varphi^*(p+y)\varphi(p-y) e^{-2ixy/\hbar} \ . \tag{3.104}$$

Moreover, we also Fourier transform the Schrödinger equation to obtain its form in momentum space. If $\hat{H}$ and $\hat{\Gamma}$ are given by some function of the momentum operator then the Fourier transform is:

$$i\hbar \frac{\partial \varphi(p)}{\partial t} = \left(\hat{H}(\hat{p}) - i\hat{\Gamma}(\hat{p})\right) \varphi(p) = \left(H(p) - i\Gamma(p)\right) \varphi(p) \ . \tag{3.105}$$

We remark that Eq. 3.104, in conjunction with the Schrödinger equation and its conjugate for the momentum wave function, give exactly the same partial time derivative obtained in the previous section, provided that we set $p \to -x$. The only changes that we need to make is to note that, when we derived in order to p in Eq. (3.96) and Eq. (3.101), we will now get an extra minus sign on the expression for the series.

This means that, for an Hermitian Hamiltonian where $\hat{H} = S(\hat{p})$, we have:

$$\frac{\partial W(x,p)}{\partial t} = \sum_{s=0}^{+\infty} \frac{1}{(2s+1)!} \frac{1}{2^{2s}} (-1)^{s+1} \hbar^{2s} \frac{\partial^{2s+1} S(p)}{\partial p^{2s+1}} \frac{\partial^{2s+1} W(x,p)}{\partial x^{2s+1}} \ . \tag{3.106}$$

And, for an anti Hermitian Hamiltonian, $\mathcal{H} = -i\hat{\Gamma}$, such that $\hat{\Gamma} = S(\hat{p})$, we have:

$$\frac{\partial W(x,p)}{\partial t} = \sum_{s=0}^{+\infty} \frac{1}{(2s)!} \frac{1}{2^{2s-1}} (-1)^{s+1} \hbar^{2s-1} \frac{\partial^{2s} S(p)}{\partial p^{2s}} \frac{\partial^{2s} W(x,p)}{\partial x^{2s}} \tag{3.107}$$

3.5.3 Summary of results

In the following table we summarize the correspondences derived so far both for Hermitian and non-Hermitian operators. In the table, the notation $\hat{\mathcal{H}} = \hat{H} - i\hat{\Gamma}$, where both $\hat{H}, \hat{\Gamma}$ are Hermitian operators, is used to specify the Hermitian and anti Hermitian parts of the Hamiltonian.

Hamiltonian	Time Evolution ($\partial_t W(x,p)$)
$\hat{H} = S(\hat{p})$	$\sum_{s=0}^{+\infty} \frac{1}{(2s+1)!} \frac{1}{2^{2s}} (-1)^{s+1} \hbar^{2s} \frac{\partial^{2s+1} S(p)}{\partial p^{2s+1}} \frac{\partial^{2s+1} W(x,p)}{\partial x^{2s+1}}$
$\hat{\Gamma} = S(\hat{p})$	$\sum_{s=0}^{+\infty} \frac{1}{(2s)!} \frac{1}{2^{2s-1}} (-1)^{s+1} \hbar^{2s-1} \frac{\partial^{2s} S(p)}{\partial p^{2s}} \frac{\partial^{2s} W(x,p)}{\partial x^{2s}}$
$\hat{H} = V(\hat{x})$	$\sum_{s=0}^{+\infty} \frac{1}{(2s+1)!} \frac{1}{2^{2s}} (-\hbar^2)^{s} \frac{\partial^{2s+1} V(x)}{\partial x^{2s+1}} \frac{\partial^{2s+1} W(x,p)}{\partial p^{2s+1}}$
$\hat{\Gamma} = V(\hat{x})$	$\sum_{s=0}^{+\infty} \frac{1}{(2s)!} \frac{1}{2^{2s-1}} (-1)^{s+1} \hbar^{2s-1} \frac{\partial^{2s} V(x)}{\partial x^{2s}} \frac{\partial^{2s} W(x,p)}{\partial p^{2s}}$

Table 3.1: Table with correspondences between operators and their contribution for the time evolution of the Wigner function

With the work done on the previous sections we are now able to write the time evolution equation for a large number of Hamiltonians, Hermitian or not. For instance if $\hat{\mathcal{H}} = \frac{\hat{p}^2}{2m} - \frac{i}{2}\hat{x}^2$ then we would get:

$$\frac{\partial W(x,p)}{\partial t} = -\frac{p}{m} \frac{\partial W(x,p)}{\partial x} - \frac{2}{\hbar} V(x) W(x,p) + \frac{\hbar}{4} \frac{\partial^2 W(x,p)}{\partial p^2} \ . \tag{3.108}$$

Furthermore, we can also confirm that for an Hermitian Hamiltonian $\hat{\mathcal{H}} = \frac{1}{2m}\hat{p}^2 + V(\hat{x})$, we reobtain the usual Wigner function time evolution equation, Eq. (2.13).

4

Numerical methods

The aim of this chapter is to describe the numerical methods used to simulate the dynamics of both wave functions and Wigner distributions under non-Hermitian Hamiltonians. Firstly, we derive a method to numerically approximate the Schrödinger evolution of a wave function when subject to a non-Hermitian Hamiltonian. We then adapt this method to be able to simulate the evolution of a Wigner function under a non-Hermitian Hamiltonian. After that, we compare how a semiclassical approximation, Eq. (3.8), performs when compared to the quantum evolution. We illustrate several examples.

4.1 Numerical method for the exact equations

In this section we describe how to computationally simulate the dynamics of the Wigner function under a NHH. The simplest possible method one may consider is to numerically simulate the Schrödinger evolution of an initial wave state. And subsequently, obtain the Wigner transformation of the wave function for each instant of time. Such algorithm has two distinct parts where numerical error can affect the accuracy of results: the numerical solution of the Schrödinger equation and the numerical integration to obtain the Wigner function from the wave function.

In order to avoid compounding numerical errors we tried to find a method which requires us to only solve the dynamics of the Wigner function. Furthermore, as most methods are only developed for Hermitian Hamiltonians, we needed to adapt the method to be able to be used with NHH.

In the following subsection we present an introduction to the split-step Fourier method [20], which can be used to numerically simulate the time propagation of a wave function.

4.1.1 Split-step Fourier method - Schrödinger's equation

The Schrödinger Equation is given by the following expression:

$$i\hbar\frac{\partial\psi(x,t)}{\partial t} = \hat{H}\psi(x,t)\ , \tag{4.1}$$

where $\psi(x,t)$ is the complex valued wave function of the system and $\hat{H}$ is the Hamiltonian of the system. A formal solution to the previous equation is:

$$\psi(x,t) = e^{-it\hat{H}/\hbar}\psi(x,0)\ . \tag{4.2}$$

If the Hamiltonian consisted of the sum of two operators, $\hat{H} = \hat{A} + \hat{B}$, such that they commute, then we could write:

$$\psi(x,t) = e^{-it\hat{A}/\hbar}e^{-it\hat{B}/\hbar}\psi(x,0)\ , \tag{4.3}$$

effectively splitting the evolution of the wave function into two separate steps. The cold truth is that, usually, $\hat{H} = \frac{\hat{p}^2}{2m} + V(\hat{x})$. This means that the two operators that make up the Hamiltonian do not commute and they cannot be easily split.

In some cases we could use the Baker-Campbell-Hausdorff formula [18] to perform this splitting:

$$\exp\left[\hat{A}\right]\exp\left[\hat{B}\right] = \exp\left[\hat{A}+\hat{B}+\frac{1}{2}\left[\hat{A},\hat{B}\right]+\frac{1}{12}\left[A,[A,B]\right]-\frac{1}{12}\left[B,[A,B]\right]+\cdots\right]\ . \tag{4.4}$$

However, numerically implementing an algorithm to perform the BCH formula on any given Hamiltonian is a rather daunting task. Thankfully, there is also another formula, called the Lie product formula or the Trotter product formula [19], which states:

$$e^{\hat{A}+\hat{B}} = \lim_{N\to+\infty}\left(e^{\hat{A}/N}e^{\hat{B}/N}\right)^N\ . \tag{4.5}$$

In the context of time evolution of a wave function, let us divide the Hamiltonian into an operator solely dependent on the momentum operator, $\hat{A}$, and another operator that depends only on the position operator, $\hat{B}$. Then the time evolution operator from $t' = 0$ to $t' = t$ can be written as:

$$e^{-it\hat{H}/\hbar} = e^{-it(\hat{A}+\hat{B})/\hbar} \approx \left(e^{-i\hat{A}t/N\hbar}e^{-i\hat{B}t/N\hbar}\right)^N + O\left(\frac{1}{2}\left[\hat{A},\hat{B}\right]\frac{t^2}{\hbar^2N^2}\right)\ . \tag{4.6}$$

Numerically, this suggests a method to perform the time evolution in increments $dt = t/N$. In each time step we would split the Hamiltonian and apply each operator to the wave function separately. By Eq. (4.4), we can see that by performing this splitting we are introducing errors on the order of $O(dt^2)$.

It remains to show how we would apply each operator separately and in a computationally efficient manner. Notice that $e^{-iV(\hat{x})t/\hbar}f(x,t)$ is a formal solution for:

$$\frac{\partial f(x,t)}{\partial t} = -\frac{i}{\hbar}V(\hat{x})f(x,t) = -\frac{i}{\hbar}V(x)f(x,t)\ . \tag{4.7}$$

As such, for operators dependent solely on the position operator we can apply the operator to the wave function simply by multiplying the wave function by a factor $\exp\left(-iV(x)dt/\hbar\right)$.

For operators dependent on the momentum operator, for example $\hat{B} = \frac{1}{2m}\hat{p}^2$, by the same logic as before we would have that the exponential of $-\frac{i}{\hbar}\hat{B}t$ is a formal solution for:

$$\frac{\partial f(x,t)}{\partial t} = -\frac{i}{2m\hbar}\hat{p}^2 f(x,t) = \frac{i\hbar}{2m}\frac{\partial^2 f(x,t)}{\partial x^2} \ . \tag{4.8}$$

We define the Fourier transform on position space of $f(x,t)$, written $\tilde{f}(k,t) = \mathcal{F}\left[f(x,t)\right]$, as:

$$\tilde{f}(k,t) = \frac{1}{\sqrt{2\pi}}\int_{-\infty}^{\infty} dx f(x,t) e^{-ikx} \ . \tag{4.9}$$

Note that wave functions must vanish at infinity meaning that, integrating by parts, we have:

$$\int_{-\infty}^{\infty} dx \frac{\partial \psi(x,t)}{\partial x} e^{-ikx} = (ik)\int_{-\infty}^{\infty} dx \psi(x,t) e^{-ikx} = (ik)\mathcal{F}\left[\psi(x,t)\right] \ . \tag{4.10}$$

The above suggests a rule for converting derivatives of wave functions into factors (ik) when passing from position space to momentum space.

If we make the Fourier transform of Eq. (4.8) we get:

$$\frac{\partial \tilde{f}(k,t)}{\partial t} = \frac{i\hbar}{2m}\int_{-\infty}^{\infty} dx \frac{\partial^2 f(x,t)}{\partial x^2} e^{-ikx} = -\frac{i\hbar}{2m}k^2 \tilde{f}(k,t) \ , \tag{4.11}$$

where in the end we used the rule derived beforehand. In momentum space, performing the action of the operator thus can be performed exactly as in the position case, just using the Fourier transform of the wave function. That is, we multiply the Fourier Transform of the function $f(x,t)$ by the factor $\exp\left(-i\hbar k^2 dt/2m\right)$.

Summing up, in order to calculate numerically the time evolution of a wave function under an Hamiltonian of the form $\hat{H} = \frac{1}{2m}\hat{p}^2 + V(\hat{x})$ we do the following:

1. We have the wave function at a specific time t, $\psi(x,t)$.
2. Fourier transform the wavefunction in the position variable and multiply it by the phase factor $e^{-\frac{i\hbar}{2m}k^2 dt}$ which is the contribution from the momentum term for the evolution;
3. Invert the Fourier Transform and multiply the wave function by the phase factor $e^{-i\frac{V(x)}{\hbar}dt}$ which is the contribution from the position term for the evolution;
4. The result is an approximation for the wave function at $t + dt$.

Algebraically we can write the above as:

$$\psi(x, t+dt) \approx e^{-i\frac{V(x)}{\hbar}dt}\mathcal{F}^{-1}\left[e^{-\frac{i\hbar}{2m}k^2 dt}\mathcal{F}\left[\psi(x,t)\right]\right] \ , \tag{4.12}$$

where $\mathcal{F}^{-1}$ denotes the inverse Fourier transform. To numerically simulate Schrödinger's time evolution we will make use of the Fourier Transform (FT) and its numerically efficient calculation method the Fast Fourier Transform (FFT), which calculates the Discrete Fourier Transform (DFT). On appendix B we make the connection between the FT and the DFT.

To be able to realize the method we have to discretize both the spatial and temporal domains. The temporal domain suffers a discretization, as previously mentioned, into steps of length dt, which influence the error due to the approximate splitting of the time evolution operator. On the other hand, to be able to apply the split operators to the function, as well as to describe the function itself, we need to discretize the position space into a grid. We use a grid that has 2^n cells, because for data in powers of two the FFT algorithm has maximum speed. This discretization also introduces errors on the functions that we try to describe on the grid, which include the operators with which we are acting on the wave function. As long as the derivatives of the functions used do not explode, we should not expect a large amount of error from this source. Furthermore, by discretizing the grid we will make it impossible for the center to have certain coordinates, like being at the point $(P, Q) = (0, 0)$, instead staying on the nearby cells. This effect will be seen on a later example.

The advantages of this method are the fact that it is easy to implement and has been shown to yield very fast results when compared to other methods, like finite-difference methods [35]. The disadvantages are that, for systems with large dispersion this method fails due to finite size effects. This disadvantage, however, does not concern us in this work as we are dealing with initial localized states, which remain localized for some period of time. As long as we do not attempt to do analysis at large periods of time we should not be concerned.

As an example of the implementation of this method, in the following image we can see a density plot of the time evolution of a wave function under the harmonic oscillator, $\hat{H} = \hat{p}^2/2 + \hat{x}^2/2$. The initial wave function is an unnormalized coherent state of the form of Eq. (2.10) where $(P, Q) = (0, 1)$, $B = i$ and we set $\hbar = 1$.

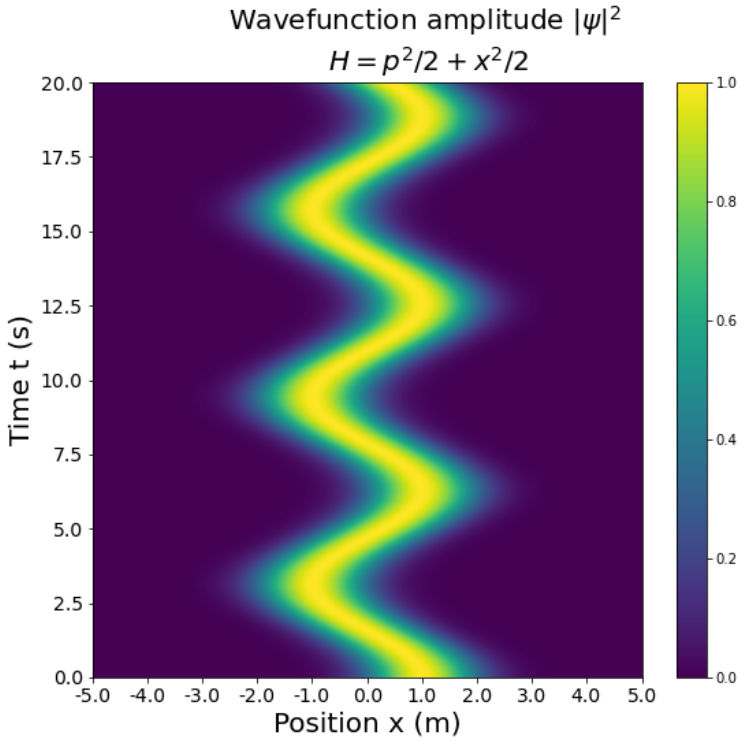

Figure 4.1: Plot of the time evolution of the probability amplitude of an initial coherent state, $|\psi(x,t)|^2$, centered at $(P,Q) = (0,1)$ and with $B = i$, under the Harmonic oscillator $\hat{H} = \hat{p}^2/2 + \hat{x}^2/2$. On the horizontal axis is the position variable. On the vertical axis is the time. The color represents the magnitude of $|\psi(x,t)|^2$. Each horizontal slice with constant t_i corresponds to a plot of $|\psi(x,t_i)|^2$.

As we can see we obtain the expected behavior for an harmonic oscillator with angular frequency $\omega = 1$. As $\omega = 1$, then the period is $T = 2\pi$. Furthermore, we see the expected motion of a coherent state under the quantum harmonic oscillator [33]. The probability amplitude simply suffers a shift with time with the center of the coherent state oscillating between $x = \pm 1$ with a period of 2π.

4.1.2 Split-step Fourier method - Wigner's distribution time evolution

The method we adopted to numerically obtain the time evolution of the Wigner function is an adaptation of the previous method. There are several uses of this method in the literature, see for example, Ref. [4] and Ref. [12].

As seen in section 3.5, the time evolution equation for an arbitrary non-Hermitian Hamiltonian, written in terms of functions and partial derivatives of the Wigner function, has a form that is highly dependent on the choice of Hamiltonian $\hat{\mathcal{H}}$. Specifically, for Hamiltonians which only depend on $\hat{p}^2$ and on potential functions $V(\hat{x})$, i.e. Hamiltonians of the form:

$$\mathcal{H} = \lambda_1 \hat{p}^2 + V(\hat{x}) - i\left(\lambda_2 \hat{p}^2 + U(\hat{x})\right) \ , \ \lambda_1, \lambda_2 \in \mathbb{R} \ , \tag{4.13}$$

we have that, using Table 3.1, the partial time derivative of the Wigner function is:

$$\begin{aligned}\frac{\partial W(p,q,t)}{\partial t} =& -2\lambda_1 p\frac{\partial W(p,q,t)}{\partial q} + \frac{\hbar\lambda_2}{2}\frac{\partial^2 W(p,q,t)}{\partial q^2} - \frac{2}{\hbar}U(q)W(p,q,t) \\ &+ \sum_{s=1}^{+\infty}\frac{1}{(2s)!}\frac{1}{2^{2s-1}}(-1)^{s+1}\hbar^{2s-1}\frac{\partial^{2s}U(q)}{\partial q^{2s}}\frac{\partial^{2s}W(p,q,t)}{\partial p^{2s}} + \\ &+ \sum_{s=0}^{+\infty}\frac{1}{(2s+1)!}\frac{1}{2^{2s}}(-\hbar^2)^s\frac{\partial^{2s+1}V(q)}{\partial q^{2s+1}}\frac{\partial^{2s+1}W(p,q,t)}{\partial p^{2s+1}}\ .\end{aligned} \tag{4.14}$$

We can see that the expression is still a linear partial differential equation. As such, we could define it as being the action of some linear operator, $\hat{Z}$, on the Wigner function. This linear operator can be decomposed into three different operators. The first, $\hat{A}$, is simply a multiplication of a function with the Wigner function, similar to the potential function term on the Schrödinger equation. The second, $\hat{B}$, which is a differential operator where the partial derivatives are with respect to position. The last one, $\hat{C}$, is simply a differential operator where the partial derivatives are with respect to momentum. In fact, as partial derivatives with respect to momentum commute with functions of the position variable we can consider the first and last operators as part of the same differential operator, i.e. $\left[\hat{A},\hat{C}\right] = 0$. From Eq. (4.14) we would see that:

$$\begin{cases}\hat{A} = -\frac{2}{\hbar}U(q) \\ \hat{B} = -2\lambda_1 p\frac{\partial}{\partial q} + \frac{\hbar\lambda_2}{2}\frac{\partial^2}{\partial q^2} \\ \hat{C} = \sum_{s=1}^{+\infty}\frac{1}{(2s)!}\frac{1}{2^{2s-1}}(-1)^{s+1}\hbar^{2s-1}\frac{\partial^{2s}U(q)}{\partial q^{2s}}\frac{\partial^{2s}}{\partial p^{2s}} + \sum_{s=0}^{+\infty}\frac{1}{(2s+1)!}\frac{1}{2^{2s}}(-\hbar^2)^s\frac{\partial^{2s+1}V(q)}{\partial q^{2s+1}}\frac{\partial^{2s+1}}{\partial p^{2s+1}}\end{cases} \tag{4.15}$$

On the previous section, we presented a method that allows one to simulate with precision the time evolution of a wave function, by splitting the time evolution operator into two factors, one acting on position space and one acting on momentum space. We will proceed in exactly the same manner to build a method for numerically obtaining the Wigner function at a later instant of time. Thus, we want to split the evolution operator into two separate exponential operators and then proceed to apply them to the Wigner function. Furthermore, because the operator that only has derivatives in order to momentum commutes with the operator that just multiplies functions of position we can perform the following split:

$$e^{\left(\hat{A}+\hat{C}\right)t} = e^{\hat{A}t}e^{\hat{C}t} = e^{\hat{C}t}e^{\hat{A}t}\ , \tag{4.16}$$

which can be seen directly from Eq. (4.4). For small time increments, $dt = T/N$, we will want to split the time evolution operator into two different operators, by making use of the Trotter formula (see Eq. (4.5)) once more:

$$e^{\hat{Z}t} = e^{\left(\hat{A}+\hat{B}+\hat{C}\right)t} \approx \left(e^{\left(\hat{A}+\hat{C}\right)\frac{t}{N}}e^{\hat{B}\frac{t}{N}}\right)^N = \left(e^{\hat{A}t/N}e^{\hat{C}t/N}e^{\hat{B}t/N}\right)^N\ . \tag{4.17}$$

Notice the equality in the last step, which implies that we can perform the act of multiplying a function with the Wigner function before or after applying the exponential of $\hat{C}$, without introducing error. However, by approximating the splitting we once again will have errors on the order of $O(dt^2)$.

With the splitting done we just need to calculate how each operator acts on the Wigner function.

The action of the exponential of the operator $\hat{A}$ is similar to the one seen in Eq. (4.7). If $\hat{A} = -\frac{2}{\hbar}U(q)$ then we just need to multiply the Wigner function by a factor $\exp\left(-2U(q)/\hbar\right)$. However, the operators $\hat{B}, \hat{C}$ are made up of derivatives of the Wigner function with respect to position and momentum, respectively. As such, we will Fourier transform the Wigner function in either the position or momentum variable to transform the derivative terms into factors of ik, where k is the frequency variable for either the position or momentum variables. Specifically, for $\hat{B}$, we Fourier transform the Wigner function on the position variable, $\tilde{W}(p,k) = \mathcal{F}_q\left[W(p,q)\right]$, where $\mathcal{F}_q$ indicates that the Fourier transform is with respect to the position variable. We assume the form for the operators as shown in Eq. (4.15), and follow the exact same procedure in deriving Eq. (4.8) and Eq. (4.11). Doing so, the action of the exponential operator $e^{\hat{B}t}$ on the Wigner function $W(p,q)$ is given by:

$$\exp\left[\left(-2\lambda_1 p(ik) + \frac{\hbar\lambda_2}{2}(ik)^2\right)t\right]\tilde{W}(p,k)\ , \tag{4.18}$$

where $\tilde{W}(p,k) = \mathcal{F}_q\left[W(q,p)\right]$. Similarly, the the action of the operator $\hat{C}$ on the Wigner function is given by:

$$\exp\left[\left(\sum_{s=1}^{+\infty}\frac{1}{(2s)!}\frac{1}{2^{2s-1}}(-1)^{s+1}\hbar^{2s-1}\frac{\partial^{2s}U(q)}{\partial q^{2s}}(ik)^{2s} + \sum_{s=0}^{+\infty}\frac{1}{(2s+1)!}\frac{1}{2^{2s}}(-\hbar^2)^s\frac{\partial^{2s+1}V(q)}{\partial q^{2s+1}}(ik)^{2s+1}\right)t\right]\tilde{W}(k,q)\ , \tag{4.19}$$

where $\tilde{W}(k,q) = \mathcal{F}_p\left[W(q,p)\right]$, i.e., the Fourier transform of $W(q,p)$ on the momentum variable.

We are now in a position to state the procedure to simulate the time evolution of a Wigner function under a NHH:

1. We start with the Wigner function at a specific time t, $W(p,q,t)$;
2. Fourier transform the Wigner function in the position variable and multiply it by the exponential factor in Eq. (4.18) where $t = dt$;
3. Invert the Fourier Transform on the position variable;
4. Fourier transform the Wigner function in the momentum variable and multiply it by the exponential factor in Eq. (4.19) where $t = dt$;
5. Invert the Fourier Transform on the momentum variable;
6. Multiply $W(p,q)$ by the exponential factor $\exp\left(-2U(q)dt/\hbar\right)$;
7. The result is an approximation for $W(p,q,t+dt)$.

Similarly to the previous section, we expect that this method is well suited for use with localized Wigner functions. For numerically propagating an initial localized Wigner functions in time, we can trust on the obtained results until the dispersion on the Wigner function is large. With this we mean, when the dispersion is such that the Wigner function starts approaching the walls of the grid used to perform the calculations, i.e. having non-zero values near the walls. When that happens, due to finite size effects, we lose precision when performing the discrete Fourier transforms. It is useful to state that this method has a run time on the order of $O(TN^2)$, where T is the total time to evolve the

state and $N = 2^n$ is the total number of cells per dimension of the grid. As for memory, the biggest contributor is the $2^n \times 2^n$ grid, with an average usage of 2^{2n+4} bytes.

We remark that we can obtain the parameter $\alpha(t)$ by integrating the Wigner function across the entire domain. The center is obtained by tracking, at each instant of time, the point of the Wigner function with highest value. As for the metric, one possible method to numerically obtain it is to numerically calculate the level curves of the Wigner function. Then, from the center point we could slide along a given level curve until we maximized the distance from the center of the state to the level curve. From the maximum, we can calculate the angle that the vector coming from the center has with the horizontal axis, thus giving us the angle α described in section 3.1. Furthermore, from the value of the wave function at the center, as well as at the point which maximizes the distance for a given level curve, we can estimate the value of the smallest eigenvalue of the coherent state, by assuming that the function is given by the Eq. (2.14). The estimate for the smallest eigenvalue is given by:

$$\exp\left(-\frac{1}{\hbar}\lambda d^2\right) = \frac{W(M)}{W(C)} \,, \tag{4.20}$$

where λ is the estimate for the smallest eigenvalue, C is the center of the Wigner function, M is the point which maximizes a previously chosen level curve and d is the distance between M and C. Then, using the calculations done in section 3.1, one could invert these relations to find the parameter B which would best describe the current Wigner function, and from which we could derive the metric via Eq.(2.15).

This algorithm for obtaining the metric was not implemented for several reasons. Firstly, the algorithm for searching for the level curves of a Wigner function would be resource intensive and would need to run almost every time step, in order to describe the motion of the metric with precision. Secondly, as we will see on the last example, when the considered system ceases to be quadratic we no longer have a well defined coherent state to which we could attribute the obtained metric. Lastly, the level curves of an initial Wigner state under a non quadratic Hamiltonian might cease to be convex. This last reason does not seem to be a problem because one could simply choose a level curve closer to the center in order to enforce convexity. However, if we try to obtain level curves closer to the center, the errors due to the discretization of space would start to greatly affect the estimate.

As an example of the implementation of the method, we again show the evolution of a coherent state under the Hermitian harmonic oscillator, $\hat{\mathcal{H}} = \frac{1}{2}\left(\hat{p}^2 + \hat{x}^2\right)$. The initial Wigner function is of the form of Eq. (2.14), with $n = 1$, $G = \mathbb{1}$ and center at $(P, Q) = (5, 0)$. We set $\hbar = 1$ and, running the simulation, at $t = 3.14$ we obtain:

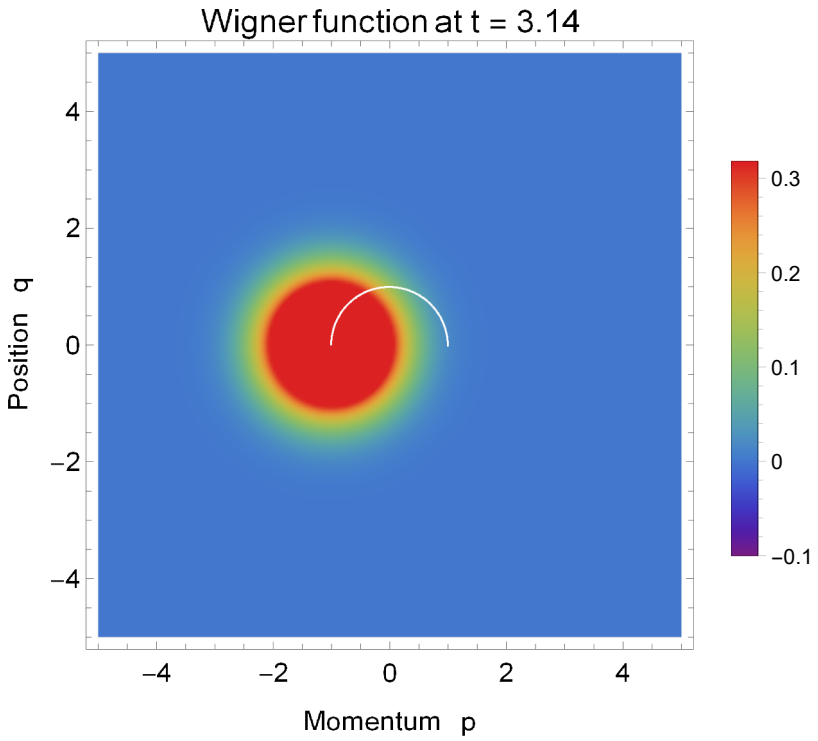

Figure 4.2: Plot of the numerical propagation of a Wigner function, $W(p, q, t)$, at a time $t = 3.14$. The time evolution is of an initial Wigner coherent state, with center at the point $(P, Q) = (1, 0)$ and metric $G = \mathbb{1}$. The Hamiltonian used was the harmonic oscillator, $\hat{\mathcal{H}} = \frac{1}{2}\left(\hat{p}^2 + \hat{x}^2\right)$. In white, we see the motion of the center from its initial point until the current time of $t = 3.14$.

In the above figure, we once again, observe the expected motion for a coherent state on phase space. The Wigner function maintains its shape across time, simply rotating around the origin. Like in the previous section, the angular frequency of the harmonic oscillator is $\omega = 1$, thus giving a period of $T = 2\pi$. This corroborates with what we see in the figure, where at approximately $t = \pi$ we see that the center completed half a rotation around the origin. In the next figure, we show the time dependence for the components of the center, for both the exact numeric propagation and the semiclassical propagation of an initial Wigner function.

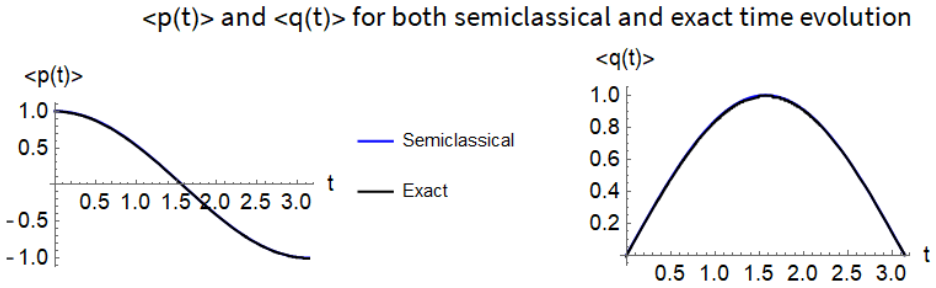

Figure 4.3: Plots for the components of the center for the exact propagation of an initial coherent Wigner function and for the semiclassical approximation. On the left is the momentum component of the center. On the right is the position component of the center. The initial Wigner coherent state has center at the point $(P, Q) = (1, 0)$ and metric $G = \mathbb{1}$.

In the above figure, we notice the sinusoidal appearance of both components of the center. Furthermore, we also remark that both curves agree completely with one another, as they effectively are

on top of each other. This is the expected behavior because the semiclassical approximation in Eq. (2.17) is exact for quadratic Hamiltonians.

In the above example, we have an Hermitian quadratic Hamiltonian, as $\hat{\Gamma} = 0$. Therefore, the example does not fully cover the possible dynamics for Wigner functions under NHH. In the next section we shall see the dynamics of two different Hamiltonians, with non zero $\hat{\Gamma}$, in more detail.

4.2 Comparing the exact Wigner time propagation with the semi-classical approximation

In this section, we shall analyze the dynamics of several non-Hermitian Hamiltonians. To achieve that, we will use the numerical propagation of a Wigner function obtained using the method developed in section 4.1. Furthermore, we shall make the comparison with the numerical solution of the system in Eq. (3.8), which yields the motion for both the center and the metric of an initial coherent Wigner state of the form of Eq.(2.14).

4.2.1 Harmonic oscillator in imaginary time

The system of equations in Eq. (3.8) was derived using second order terms of the time evolution equation for the Wigner function. As such, the semiclassical approximation, i.e. Eq. (3.8), is exact for any quadratic non-Hermitian Hamiltonian. Nevertheless, we shall explicitly confirm that with this example.

We take as our Hamiltonian:

$$\hat{\mathcal{H}} = -\frac{i}{2}\left(\hat{p}^2 + \hat{x}^2\right) \implies \begin{cases} \hat{H} = 0 \\ \hat{\Gamma} = \frac{1}{2}\left(\hat{p}^2 + \hat{x}^2\right) \end{cases}, \tag{4.21}$$

which is the usual harmonic oscillator but evolving in imaginary time. In section 3.4, we solved analytically Eq. (3.8) for a Wigner coherent state with initial metric G diagonal. As such, to further corroborate the results found, we too, in this example, shall assume that the initial Wigner coherent state, of the form of Eq. (2.14) has $G = \mathrm{diag}(\frac{1}{2}, 2)$ and center $(P, Q) = (2, 0)$. The results obtained are displayed in the following figure:

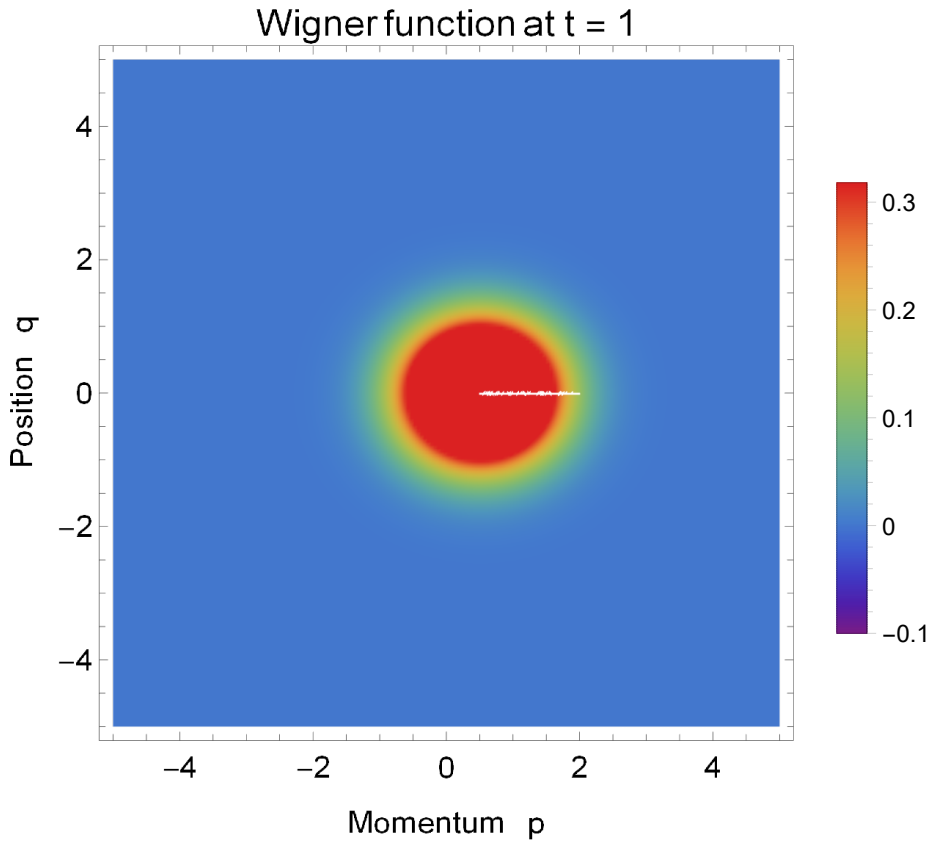

Figure 4.4: Plot of the numerical propagation of a Wigner function, $W(p, q, t)$, at a time $t = 1$. The time evolution is of an initial Wigner coherent state, with center at the point $(P, Q) = (2, 0)$ and metric $G = \mathrm{diag}(1/2, 2)$. The Hamiltonian used was the anti Hermitian harmonic oscillator, $\hat{\mathcal{H}} = -\frac{i}{2}\left(\hat{p}^2 + \hat{x}^2\right)$. In white, we see the motion of the center from its initial point until the current time.

In the above figure we can observe that, an initial state which was larger in the momentum direction than in the position direction, moved towards the origin whilst the shape of the localized state became uniform. This behavior was exactly the predicted one in subsection 3.4.3. As a matter of fact, looking at figure 3.5, we can see that, at $t = 1$, the momentum component of the center should be roughly at $P = 0.5$. This is also seen on the next figure, where the momentum and position components of the center are plotted. The next plot includes both the exact numeric propagation as well as the semiclassical numeric solution arising from Eq. (2.17).

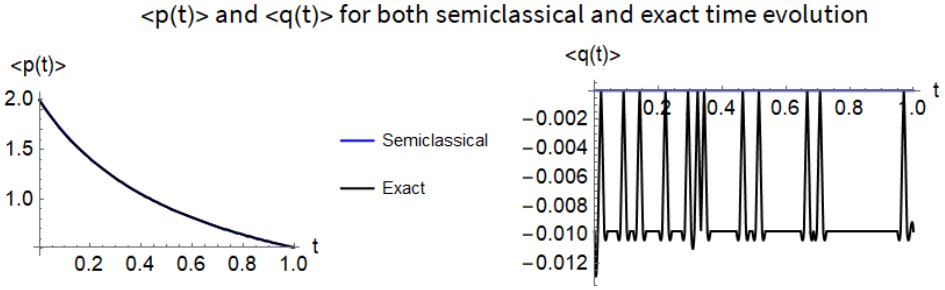

Figure 4.5: Plots for the components of the center for the exact propagation of an initial coherent Wigner function and for the semiclassical approximation. On the left is the momentum component of the center. On the right is the position component of the center. The initial Wigner coherent state has center at the point $(P, Q) = (2, 0)$ and metric $G = \mathrm{diag}(\frac{1}{2}, 2)$.

In the above plot, we confirm that the motion for the momentum component of the center is in agreement with the one predicted by the semiclassical approximation in Eq. (2.17). However, it is noteworthy to discuss what is happening on the plot of the position component of the center. The particular spatial discretization chosen for this example was a 1024×1024 grid. Thus, the length of each cell is $\frac{1}{1024} \approx 10^{-2}$. As the system cannot numerically be at zero, due to the spatial discretization, the position component stays on the cell/cells closest to the origin. This is further corroborated by the fact that, if we do increase the size of the grid, say, by a factor of two, then the plot on the right side is very similar to the present one but with the center being away from the origin by $\frac{1}{2048}$.

4.2.2 Quartic oscillator with damping

We now proceed to numerically simulate the Hamiltonian in Eq. (2.21), $\hat{\mathcal{H}} = \left(\frac{1}{2} - i\frac{1}{10}\right)(\hat{p}^2 + \hat{q}^2) + \frac{1}{8}\hat{q}^4$, in order to check if we obtain the same dynamics using the method developed in this section.

As such, we consider an initial Wigner state with center $(P, Q) = (5, 0)$ and initial metric $G = \mathbb{1}$. We numerically propagated the state and we also numerically solved Eq. (3.8), with the help of *Mathematica*. At $t = 2.5$ we observe:

Figure 4.6: Plots of the numerical and semiclassical propagation of a Wigner function, $W(p, q, t)$, at a time $t = 2.5$ and for $\hbar = 1$. The time evolution is of an initial Wigner coherent state, with center at the point $(P, Q) = (5, 0)$ and metric $G = \mathbb{1}$. The Hamiltonian used was $\hat{\mathcal{H}} = \left(\frac{1}{2} - i\frac{1}{10}\right)(\hat{p}^2 + \hat{q}^2) + \frac{1}{8}\hat{q}^4$.

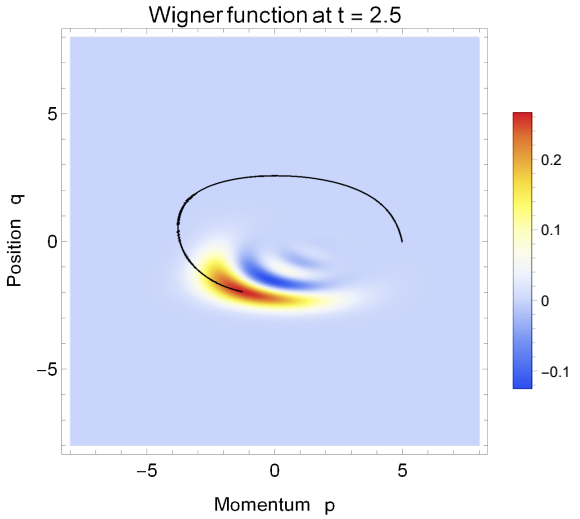

(a) Density plot of the numerical propagation of the Wigner function. In black, we see the motion of the center from its initial point until the current time.

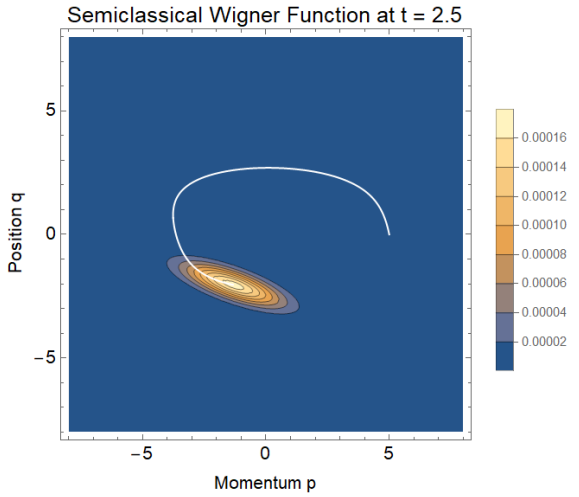

(b) Contour plot of the numerical solutions to Eq. (3.8). In white, we see the motion of the center from its initial point until the current time.

We can compare the above figures to the middle figures in Fig. 2.1 and the behavior displayed on both appears to be the same. The Hamiltonian considered was an Hermitian quartic oscillator with an additional anti-Hermitian harmonic term. As such, the expected motion would be an oscillation around the origin, with some changes due to the quartic part. On the next picture we can observe the comparison between the components of the center for the exact solution of the Wigner dynamic equation and for the semiclassical approximation:

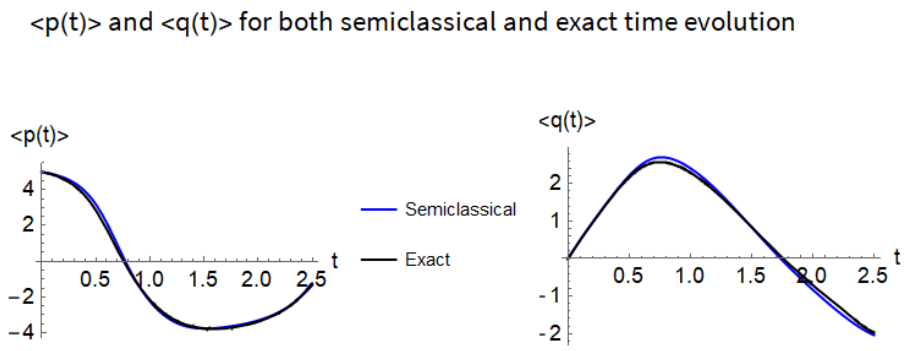

Figure 4.7: Plots for the components of the center for the exact propagation of an initial coherent Wigner function and for the semiclassical approximation. On the left is the momentum component of the center. On the right is the position component of the center. The initial Wigner coherent state has center at the point $(P, Q) = (5, 0)$ and metric $G = \mathbb{1}$.

As we can see, the semiclassical approximation agrees with the motion of both components of the center, as one could also infer from Fig. 4.6. As we analyzed in section 3.4, the behavior of the harmonic oscillator in imaginary time is to drive the state towards the origin and to quickly decrease the parameter $\alpha(t)$. For the exact numerical propagation, we can obtain the parameter $\alpha(t)$ by integrating the Wigner function across all the domain, using Simpson's rule. Doing so leads to the following plot:

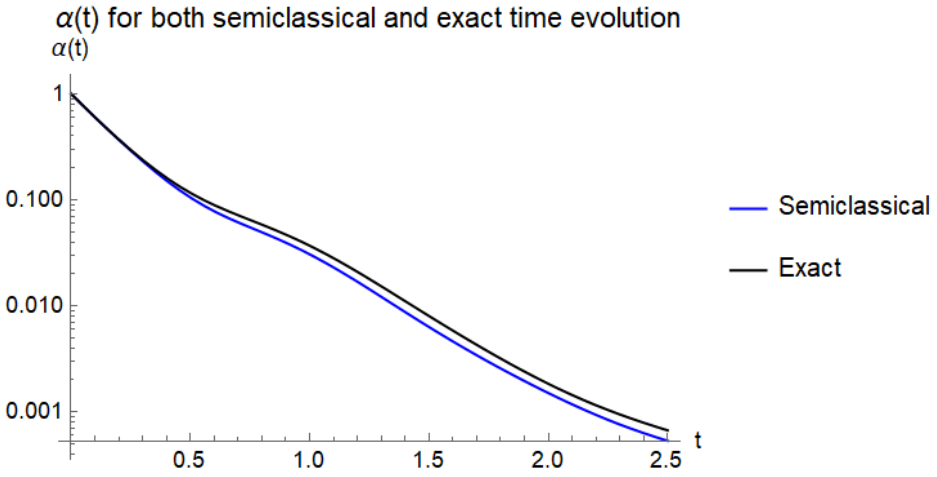

Figure 4.8: Logarithmic plot for the parameter $\alpha(t)$ of a Wigner function. The initial Wigner coherent state has center at the point $(P, Q) = (5, 0)$ and metric $G = \mathbb{1}$. We also set $\hbar = 1$. In blue we see the $\alpha(t)$ for the semiclassical numerical solution to Eq. (3.8). In black we see $\alpha(t)$ for the numerical propagation of the initial Wigner state.

We once again corroborate the results in Fig. 2.1, the semiclassical approximation is in general agreement with the $\alpha(t)$ obtained for the exact numerical propagation of the initial Wigner function. However, this agreement is not surprising. This is due to the fact that the major contributor for the loss of wavefunction norm is $\hat{\Gamma}(p, q)$, as can be seen on the last equation in Eq. (3.8).

5

Connecting stochastic differential equations and non-Hermitian Hamiltonians

In this chapter, based in Ref. [6] , we will establish a connection between the formalism of stochastic optimization of a certain class of control systems and quantum non-Hermitian Hamiltonians. By solving Eq. (2.17), the non-Hermitian semiclassical dynamics of the center and metric of Gaussian wave packets can be found. An example of a quadratic Hamiltonian is then explored.

5.1 From the HJB equation to a Schrödinger-like equation - 1 dimensional case

In one dimension, for both the state and the control, equation (2.32) reads:

$$-\hbar\frac{\partial}{\partial t}\psi = \frac{1}{2}\hbar^2 A_t \Delta\left(\psi_t\right) + \hbar f_t\left(\frac{\partial}{\partial x}\psi_t\right) - q(x)\psi_t \ , \tag{5.1}$$

where $A_t = G_t R^{-1} G_t$ and $\Delta = \frac{\partial^2}{\partial x^2}$. We remark that, in this section, the index in order to time means that a variable may depend on the state x_t and/or explicitly on time. The above equation can be rewritten with the change $t \to -s$ as:

$$\hbar\frac{\partial}{\partial s}\psi_s = \hbar^2 A(x_s)\frac{\Delta}{2}\psi_s + \hbar f(x_s)\left(\frac{\partial}{\partial x}\psi_s\right) - q(x_s)\psi_s \ , \tag{5.2}$$

implying that the wave function at an instant s is given by:

$$\psi_s = \exp\left[\frac{s}{\hbar}\left(\hbar^2\frac{A(x)\Delta}{2} + \hbar f_s\partial_x - q(x)\right)\right]\psi_0 \tag{5.3}$$

We can identify a non-Hermitian Hamiltonian in the above expression by rewriting it as:

$$\psi_s = \exp\left[-\frac{i}{\hbar}s\left(i\hbar f\partial_x + i\left(\hbar^2 A(x)\frac{\Delta}{2} - q(x)\right)\right)\right]\psi_0 \tag{5.4}$$

Thus the non-Hermitian Hamiltonian is given by:

$$\hat{\mathcal{H}} = -f(\hat{x})\hat{p} - iA(\hat{x})\frac{(\hat{p})^2}{2} - iq(\hat{x}) = -\left(f(\hat{x})\hat{p}\right) - i\left(\frac{A(\hat{x})(\hat{p})^2}{2} + q(\hat{x})\right) \tag{5.5}$$

5.1.1 Obtaining the classical Hamiltonian

To be able to apply the previous formalism, we must be able to obtain the classical Hamiltonian from the quantum one to solve the semiclassical dynamics. In order to do that, we will assume that the quantization of a classical observable is given by the symmetric quantization scheme i.e., we assume that the quantization of a classical function $f(x)g(p)$ is $f(x)g(p) \to \frac{1}{2}\left(f(\hat{x})g(\hat{p}) + g(\hat{p})f(\hat{x})\right)$. Under this choice of quantization we get that functions of solely the position or momentum variable correspond to operators that solely depend on the position or momentum operator.

In the Schrödinger representation, we assume that the quantization of the function $F = f(x)p$ is thus given by the symmetric quantization, i.e.:

$$\hat{F} = -\frac{1}{2}f(x)i\hbar\partial_x - \frac{i\hbar}{2}\partial_x \circ f(x) = f(\hat{x})\hat{p} - \frac{i\hbar}{2}f'(\hat{x}) \tag{5.6}$$

Thus the quantization of the classical observable $G = f(x)p + \frac{i\hbar}{2}f'(x)$ is given by:

$$\hat{G} = f(\hat{x})\hat{p} \tag{5.7}$$

It remains to be shown which classical observable gives us the operator $\widehat{A(x)p^2}$. We note that the quantization of the classical observable $f(x)p^2$ under our choice of quantization scheme is:

$$\widehat{(f(x)p^2)} = -\frac{1}{2}\hbar^2 f(x)\partial_x^2 - \frac{1}{2}\hbar^2\partial_x^2 \circ f(x) = f(\hat{x})\hat{p}^2 - i\hbar f'(\hat{x})\hat{p} - \frac{1}{2}\hbar^2 f''(\hat{x}) \tag{5.8}$$

Thus joining the previous result it follows that the quantization of the following classical observable is:

$$O = f(x)p^2 + i\hbar f'(x)p \implies \hat{O} = f(\hat{x})\hat{p}^2 \tag{5.9}$$

And so our quantum Hamiltonian arises from the quantization of the classical observable:

$$\mathcal{H} = -f(x)p - \frac{i\hbar}{2}f'(x) - \frac{i}{2}\left(A(x)p^2 + i\hbar A'(x)p\right) - iq(x)\ , \tag{5.10}$$

from where we identify:

$$\begin{cases} H = \left(\hbar\frac{A'(x)}{2} - f(x)\right)p \\ \Gamma = \frac{A(x)(p)^2}{2} + \left(\hbar\frac{f'(x)}{2} + q(x)\right) \end{cases} \tag{5.11}$$

The evolution of the above system of equations can be thus evaluated using the formalism developed in the previous chapters. In the next section we explore a simple example, with a complex quadratic Hamiltonian.

5.2 Example - Quadratic Hamiltonian

In this section we will work with following stochastic differential equation:

$$\dot{x} = -\alpha x + (u_t + \xi) \ , \tag{5.12}$$

where ξ has variance δ so that we have $A_t = \delta$. The parameter α controls the linear drift and the parameter δ controls the noise. We can think of Eq. (5.12) as an exponentially decaying system that can be influenced via the control u_t and its associated noise ξ.

Moreover, we also take as a cost function a quadratic function of the following form:

$$r_t = q(x) + \frac{1}{2}Ru^2 = \frac{\beta}{2}x^2 + \frac{1}{2}\frac{\hbar}{\delta}u^2 \tag{5.13}$$

With the above assumptions, and following Eq. (5.11), we get the following classical Hamiltonian function:

$$\begin{cases} H = \alpha x p \\ \Gamma = \frac{\delta}{2}p^2 + \frac{\beta}{2}x^2 - \frac{\alpha\hbar}{2} \end{cases} . \tag{5.14}$$

Looking at Eq. (2.30), if the value function at $t = 0$ is quadratic then we must have an initial state that is localized and purely real, i.e., a Gaussian which is centered at a point $Y = (0, x_0)$:

$$\psi_s = \left(\frac{b}{\pi\hbar}\right)^{\frac{1}{4}} \exp\left[-\frac{b}{2\hbar}(x - x_0)^2\right] \ . \tag{5.15}$$

The above corresponds to have a given final cost that is a quadratic function of the state. Furthermore, by evolving this Wigner function using Eqs. (2.17), we are able to obtain the evolution for the value function as well, which will be given by the logarithm of our wave function. We remark that, under this formalism, the value function, which is a real function, evolves through a wave function under a non-Hermitian Hamiltonian, which is somewhat unexpected.

Looking at the Hamiltonian in Eqs. (5.14) and at the second equation in (2.17), assuming an initial diagonal metric of the form:

$$G(t = 0) = \begin{pmatrix} g_1(t = 0) & 0 \\ 0 & g_2(t = 0) \end{pmatrix} \ ,$$

then we obtain the following equation for the metric components:

$$\dot{g_1}(t) = \delta + 2\alpha g_1(t) - \beta g_1(t)^2 \ ,$$
$$\dot{g_2}(t) = \beta - 2\alpha g_2(t) - \delta g_2(t)^2 \ .$$

One can then verify that if we define $g_2(t) = 1/g_1(t)$, we obtain the second equation from the first one and vice-versa. This implies that if the initial conditions for the metric are such that its determinant is equal to one, then, for all time t, the same is true, and the components are inverse of each other. This also implies that we only need to solve one differential equation to get the complete time evolution of the metric.

The above remark is valid only in the case of quadratic Hamiltonians of the form of (5.14). For example, if we had a real component quadratic in position, then we would not only lose the above property but metric would no longer be diagonal for a generic time t .

For the rest of this section we will analyze the Hamiltonian in (5.14) in three different cases:

- First the case $\alpha = \beta = 0$ with $\delta \neq 0$;
- Secondly, the case $\alpha = 0$ and $\beta \neq 0, \delta \neq 0$;
- Lastly, the case where $\alpha \neq 0$, $\beta \neq 0$, $\delta \neq 0$,

and for the last case we shall see what is the role of the several parameters on the behavior of the metric and position of the center of the wave packet. To avoid confusion with the parameter α of the Hamiltonian, for the rest of this section we will denote the multiplicative factor, described by the third equation in Eqs. (2.17), by $N(t)$.

5.2.1 Quadratic only in momentum

We consider the system of (5.14) where we put $\alpha = \beta = 0$ and $\delta \neq 0$. Thus, our classical Hamiltonian is given by:

$$\begin{cases} H = 0 \\ \Gamma = \frac{\delta p^2}{2} \end{cases} \tag{5.16}$$

This is a purely imaginary quadratic Hamiltonian that only depends on momentum. We take an initial Gaussian state which is centered at a point $Y = (0, x_0)$:

$$\psi_s = \left(\frac{b}{\pi\hbar}\right)^{\frac{1}{4}} \exp\left[-\frac{b}{2\hbar}(x - x_0)^2\right] \ , \tag{5.17}$$

from where we see that $B = ib \in i\mathbb{R}$. Thus, the Wigner function for this wave function has initial center at the origin $Y = (0, x_0)$ and with $G = \begin{pmatrix} \frac{1}{b} & 0 \\ 0 & b \end{pmatrix}$.

In this case the equation for G is independent of Y and is an equation of the following form:

$$\dot{G} = \begin{pmatrix} \delta & 0 \\ 0 & 0 \end{pmatrix} - G \begin{pmatrix} 0 & 0 \\ 0 & \delta \end{pmatrix} G \ , \tag{5.18}$$

where, as the Hamiltonian is quadratic, this implies that one of the components of the metric is the inverse of the other. It thus suffices to calculate the momentum related component:

$$\dot{g}(t) = \delta \implies \delta t + \frac{1}{b} \,, \tag{5.19}$$

where we already took into account the initial conditions for the metric. This result implies that the metric is given by:

$$G(t) = \begin{pmatrix} \delta t + \frac{1}{b} & 0 \\ 0 & \left(\delta t + \frac{1}{b}\right)^{-1} \end{pmatrix} \,. \tag{5.20}$$

Furthermore, the center's equation of motion is given by:

$$\dot{Y} = -G(t)^{-1} \nabla \Gamma(Y) \,, \tag{5.21}$$

which can be written as:

$$\frac{\dot{p}}{p} = -\frac{1}{t + \frac{1}{\delta b}} \tag{5.22}$$

$$\dot{x} = 0 \,. \tag{5.23}$$

Integrating the above equations thus give us:

$$p(t) = \frac{p(0)}{1 + \delta b t} \tag{5.24}$$

$$x(t) = x(0) \,, \tag{5.25}$$

where the initial conditions for the position and momentum are taken into account. As we have that the initial center is $Y = (0, x_0)$, we see that the center will not move, remaining constant for all time.

Moreover, for large time we observe that the metric tends to the matrix:

$$G_\infty = \begin{pmatrix} +\infty & 0 \\ 0 & 0 \end{pmatrix} \,. \tag{5.26}$$

Furthermore, knowing the evolution of the metric and the center it is thus possible to calculate the evolution of the multiplicative factor of the wave packet using (2.17). In this case it is of the form:

$$N(t) = \frac{N_0}{\sqrt{b\delta t + 1}} \,, \tag{5.27}$$

where N_0 is the initial multiplicative factor (normalization constant).

5.2.2 Quadratic in position and momentum

We now consider the system of (5.14) in the case where $\alpha = 0$ and $\beta \neq 0, \delta \neq 0$. Thus, our classical Hamiltonian is given by:

$$\begin{cases} H = 0 \\ \Gamma = \frac{\delta p^2}{2} + \frac{\beta x^2}{2} \end{cases} \tag{5.28}$$

Again, this is a purely imaginary Hamiltonian and its dynamics can be seen as the purely imaginary

time evolution of a regular Hermitian Hamiltonian. We take as the initial state the following Gaussian which is centered at a given point:

$$\psi_s = \left(\frac{b}{\pi\hbar}\right)^{\frac{1}{4}} \exp\left[-\frac{b}{2\hbar}(x-x_0)^2\right] , \tag{5.29}$$

from where we see that $B = ib \in i\mathbb{R}$. The Wigner function for this wave function has initial center at the point $Y = (0, x_0)$ and with $G = \begin{pmatrix} \frac{1}{b} & 0 \\ 0 & b \end{pmatrix}$.

In this case the equation for G is independent of Y and is a Ricatti equation:

$$\dot{G} = \begin{pmatrix} \delta & 0 \\ 0 & \beta \end{pmatrix} - G \begin{pmatrix} \beta & 0 \\ 0 & \delta \end{pmatrix} G . \tag{5.30}$$

Once more it suffices to solve the differential equation for the momentum component of the metric:

$$\dot{g}(t) = \delta - \beta g(t)^2 \implies g(t) = \frac{b\delta \sinh\left(t\sqrt{\beta\delta}\right) + \sqrt{\beta\delta}\cosh\left(t\sqrt{\beta\delta}\right)}{b\sqrt{\beta\delta}\cosh\left(t\sqrt{\beta\delta}\right) + \beta\sinh\left(t\sqrt{\beta\delta}\right)} , \tag{5.31}$$

where the initial conditions were already taken into account.

The metric is thus given by:

$$G(t) = \begin{pmatrix} g(t) & 0 \\ 0 & (g(t))^{-1} \end{pmatrix} . \tag{5.32}$$

Furthermore, the center's equation of motion is given by:

$$\frac{\dot{p}}{p} = -\delta\,(g(t))^{-1} \tag{5.33}$$

$$\frac{\dot{x}}{x} = -\beta g(t) \tag{5.34}$$

Integrating the above equations and using the initial condition that $Y = (0, x_0)$ thus give us:

$$p(t) = 0 \tag{5.35}$$

$$x(t) = \frac{bx_0\sqrt{\beta\delta}}{b\sqrt{\beta\delta}\cosh\left(t\sqrt{\beta\delta}\right) + \beta\sinh\left(t\sqrt{\beta\delta}\right)}, \tag{5.36}$$

For large time we observe that the center Y tends to the origin $Y_\infty = (0, 0)$. Moreover, the metric tends to the matrix:

$$G_\infty = \begin{pmatrix} \sqrt{\frac{\delta}{\beta}} & 0 \\ 0 & \sqrt{\frac{\beta}{\delta}} \end{pmatrix} \tag{5.37}$$

As for the multiplicative factor, we obtain:

$$N(t) = -\sqrt{8}N_0\sqrt[4]{-b^2\beta}\left(b^2(-\delta) + \left(\beta - b^2\delta\right)\cosh\left(2t\sqrt{\beta\delta}\right) - \beta\right)^{3/4}\left(b^2\delta + \left(\beta - b^2\delta\right)\cosh\left(2t\sqrt{\beta\delta}\right) + \beta\right)^{3/4}\cdot$$
$$\cdot\sqrt[4]{1 - \frac{b\delta\tanh\left(t\sqrt{\beta\delta}\right)}{\sqrt{\beta\delta}}}\sqrt[4]{\delta - \frac{\sqrt{\beta\delta}\tanh\left(t\sqrt{\beta\delta}\right)}{b}}\exp\left(-\frac{b\beta x_0^2}{b\hbar\sqrt{\beta\delta}\coth\left(t\sqrt{\beta\delta}\right) + \beta\hbar}\right)\Big/$$
$$\Big/\left(6\beta b^2\delta + b^4\delta^2 - \left(\beta - b^2\delta\right)^2\cosh\left(4t\sqrt{\beta\delta}\right) + \beta^2\right)\sqrt[4]{\frac{\beta\tanh\left(t\sqrt{\beta\delta}\right)}{b\sqrt{\beta\delta}} + 1}\sqrt[4]{\frac{b\delta\tanh\left(t\sqrt{\beta\delta}\right)}{\sqrt{\beta\delta}} + 1}$$

5.2.3 Quadratic with linear mixed term

We now consider the system of (5.14) in the case where $\alpha = 0$ and $\beta \neq 0, \delta \neq 0$. Thus, our classical Hamiltonian is given by:

$$\begin{cases} H = \alpha x p \\ \Gamma = \frac{\delta p^2}{2} + \frac{\beta x^2}{2} - \frac{\alpha \hbar}{2} \end{cases} \tag{5.38}$$

Where the Hamiltonian is now no longer purely imaginary being instead complex. We again take as the initial state the following Gaussian:

$$\psi_s = \left(\frac{b}{\pi\hbar}\right)^{\frac{1}{4}} \exp\left[-\frac{b}{2\hbar}(x - x_0)^2\right] , \tag{5.39}$$

from where we see that $B = ib \in i\mathbb{R}$. The Wigner function for this wave function has initial center at the origin $Y = (0, x_0)$ and with $G = \begin{pmatrix} \frac{1}{b} & 0 \\ 0 & b \end{pmatrix}$.

Let us now solve this problem using the method described in subsection 3.3.2. We have that:

$$-X_{\mathcal{H}} = (\alpha p - i\beta x)\frac{\partial}{\partial p} + (i\delta p - \alpha x)\frac{\partial}{\partial x} . \tag{5.40}$$

And so, we have:

$$\begin{cases} p_t = e^{-X_{\mathcal{H}} t} p \implies \dot{p}_t = e^{-X_{\mathcal{H}} t}\left(-X_{\mathcal{H}} p\right) = \alpha p_t - i\beta x_t \\ x_t = e^{-X_{\mathcal{H}} t} x \implies \dot{x}_t = e^{-X_{\mathcal{H}} t}\left(-X_{\mathcal{H}} x\right) = -\alpha x_t + i\delta p_t \end{cases} , \tag{5.41}$$

which can be written in matrix form as:

$$\begin{pmatrix} \dot{p}_t \\ \dot{x}_t \end{pmatrix} = \begin{pmatrix} \alpha & -i\beta \\ i\delta & -\alpha \end{pmatrix} \begin{pmatrix} p_t \\ x_t \end{pmatrix} . \tag{5.42}$$

This is a matrix differential equation of the form $\dot{\boldsymbol{v}}_t = M\boldsymbol{v}_t$. The solution is thus given by the matrix exponential, $\boldsymbol{v}_t = e^{Mt}\boldsymbol{v}_0$. The matrix exponential can be obtained by diagonalizing the matrix $M = UDU^{-1}$ and calculating $e^{Mt} = Ue^{Dt}U^{-1}$. In this case, the matrix has eigenvalues:

$$\lambda_{\pm} = \pm\sqrt{\alpha^2 + \beta\delta} , \tag{5.43}$$

and so, denoting by λ the positive eigenvalue, we obtain the following matrix exponential:

$$e^{Mt} = \begin{pmatrix} \cosh(\lambda t) + \frac{a}{\lambda}\sinh(\lambda t) & -i\frac{b}{\lambda}\sinh(\lambda t) \\ i\frac{d}{\lambda}\sinh(\lambda t) & \cosh(\lambda t) - \frac{a}{\lambda}\sinh(\lambda t) \end{pmatrix} . \tag{5.44}$$

Taking into account the starting metric $G = \mathrm{diag}(\frac{1}{b}, b)$ we have the following initial holomorphic coordinate:

$$z_0 = p - ibx , \tag{5.45}$$

and so applying the flow of the Hamiltonian vector field we get:

$$z_t = p\left(\cosh(\lambda t) + \frac{\alpha + b\delta}{\lambda}\sinh(\lambda t)\right) - ibx\left(\cosh(\lambda t) + \frac{\beta/b - \alpha}{\lambda}\sinh(\lambda t)\right) := p_t - ibx_t \tag{5.46}$$

And so we have that:

$$\tilde{\varphi}_t^{-X_{\mathcal{H}}} = \begin{pmatrix} \cosh(\lambda t) + \frac{\alpha+b\delta}{\lambda}\sinh(\lambda t) & 0 \\ 0 & \cosh(\lambda t) + \frac{\beta/b-\alpha}{\lambda}\sinh(\lambda t) \end{pmatrix} . \tag{5.47}$$

From the inverse of the above we thus conclude that the center motion is given by:

$$\begin{cases} P(t) = \frac{P(0)}{\cosh(\lambda t)+\frac{\alpha+b\delta}{\lambda}\sinh(\lambda t)} = 0 \\ X(t) = \frac{X(0)}{\cosh(\lambda t)+\frac{\beta/b-\alpha}{\lambda}\sinh(\lambda t)} = \frac{\lambda b X(0)}{\lambda b\cosh(\lambda t)+(\beta-b\alpha)\sinh(\lambda t)} \end{cases} \tag{5.48}$$

Finally, we can obtain the metric by first obtaining the complex structure directly from Eq. (5.46). And so, as mentioned in subsection 3.3.3, a scaling of the holomorphic does not alter the inherent complex structure. In this case we can divide the entire equation by the real factor of the x coordinate to directly obtain $g(t)$ as the coefficient of the p coordinate. We thus have:

$$g(t) = \frac{\lambda\cosh(\lambda t) + (\alpha + b\delta)\sinh(\lambda t)}{b\lambda\cosh(\lambda t) + (\beta - b\alpha)\sinh(\lambda t)} , \tag{5.49}$$

where $\lambda = \sqrt{\alpha^2 + \beta\delta}$. We note that we can reobtain the previous equations by simply setting any of the α, β, δ to zero.

For large time we observe that the center Y tends to the origin $Y_\infty = (0, 0)$. And for large time the metric tends to the matrix:

$$G_\infty = \begin{pmatrix} \frac{\sqrt{\alpha^2+\beta\delta}+\alpha}{\beta} & 0 \\ 0 & \left(\frac{\sqrt{\alpha^2+\beta\delta}+\alpha}{\beta}\right)^{-1} \end{pmatrix} , \tag{5.50}$$

where the dependence in b is not present. Thus, in the infinite time limit, the system forgets its initial geometry, which is related to the b parameter.

As for the multiplicative factor, solving the last equation in 2.17 yields the expression for the $N(t)$ written in appendix D.

5.2.4 Center and metric behavior with change of parameters

In this subsection we shall see the role of the parameters α, β, δ on the time evolution of the momentum component of the metric and of the center's position. In all the below images the darker the coloring of the curve the smaller the value of the parameter being used to plot said curve.

5.2.4.A Influence of parameter α

The parameter α is associated with the linear drag on equation (5.12). In the next image we can see its influence on the momentum component of the metric, where we see that it controls the limit to which this components tends to, while maintaining all the other parameters fixed. The bigger the parameter the larger the limit this metric component tends to.

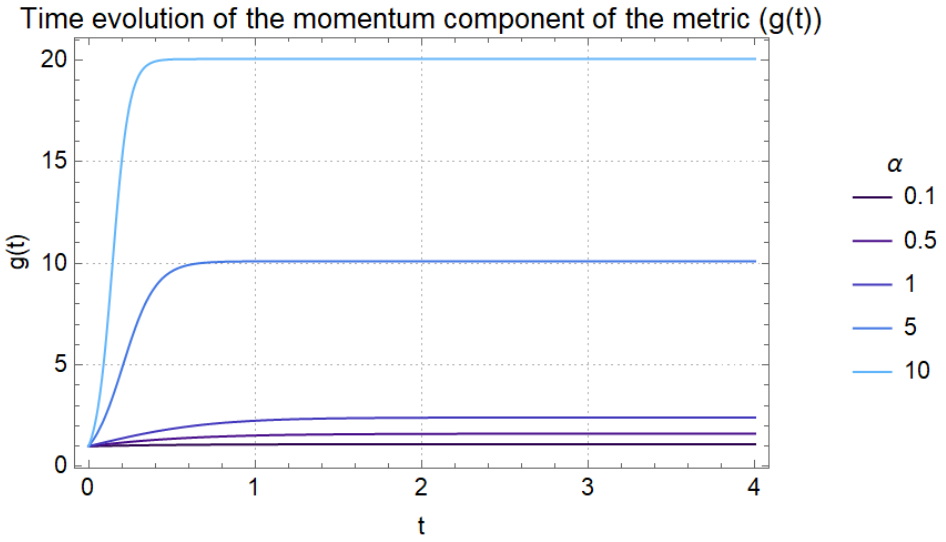

Figure 5.1: Momentum metric component g(t) for different values of α where $\beta = \delta = b = 1$

Whereas on the center's position, displayed in the next image on the left side, we can see that the parameter α controls the height of the peak of maximum distance from the origin that the center has before tending to the origin. As for the role of the parameter α on the evolution of the multiplicative factor we see that it is similar to the one in the position case, being responsible for a deviation from the origin, for big enough values of α.

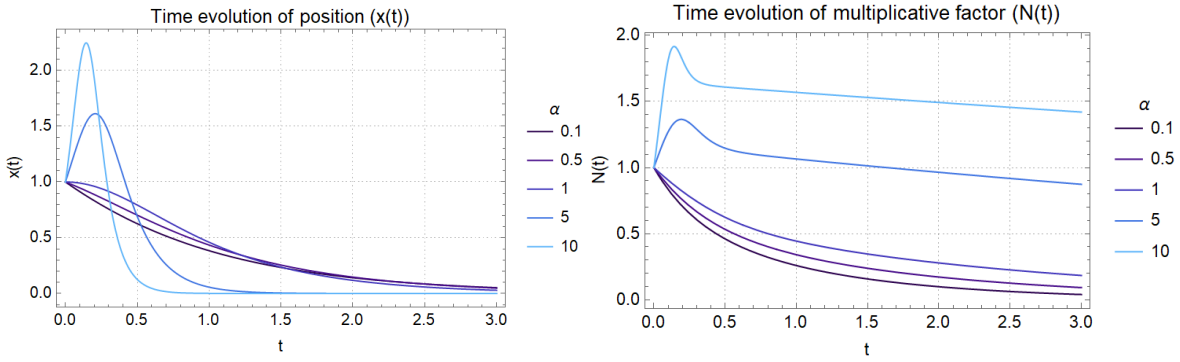

(a) Center's position x(t) for different values of α where $\beta = \delta =$ $b = x_0 = 1$

(b) Multiplicative factor N(t) for different values of α where $\beta = \delta = b = x_0 = N_0 = \hbar = 1$

Figure 5.2: Influence of the parameter α on the time evolution for position of the center of the wave packet (left image) and for the multiplicative factor (right image)

5.2.4.B Influence of parameter β

The parameter β is associated with the quadratic term on the position, that appears due to our choice of the cost function in (5.13). In the next image we can see its influence on the momentum component of the metric, where we see that it controls the limit to which this components tends to. This limit is smaller for large values of this β.

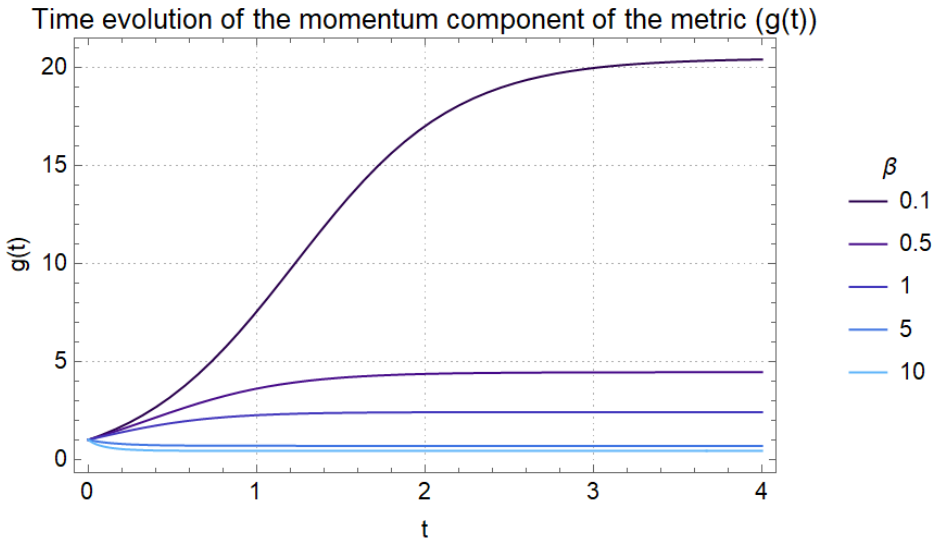

Figure 5.3: Momentum metric component g(t) for different values of β where $\alpha = \delta = b = 1$

Whereas on the center's position, displayed in the next image on the left side, we can see that the parameter β also controls the height of the peak of maximum distance from the origin that the center has before tending to the origin but in a manner opposite to the parameter α. The smaller β is, the bigger this peak becomes. The same can be said for the influence of β on the evolution of the multiplicative factor.

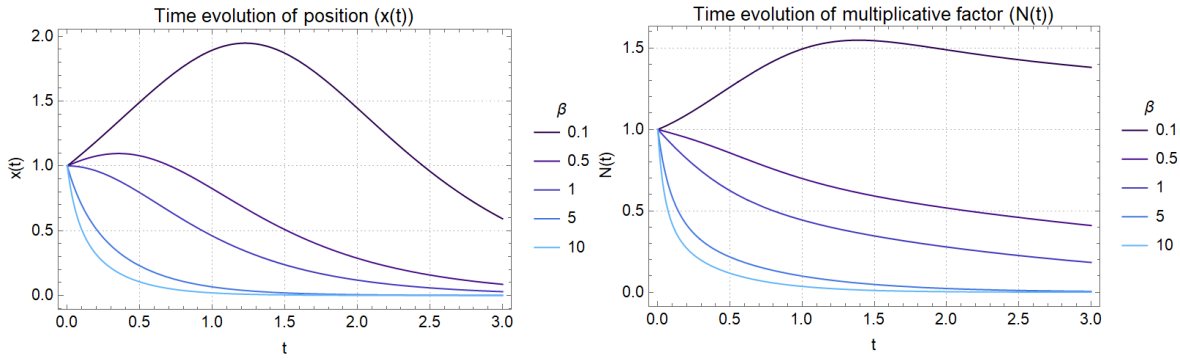

(a) Center's position x(t) for different values of β where $\alpha = \delta =$ $b = x_0 = 1$

(b) Multiplicative factor N(t) for different values of β where $\alpha = \delta = b = x_0 = N_0 = \hbar = 1$

Figure 5.4: Influence of the parameter β on the time evolution for position of the center of the wave packet (left image) and for the multiplicative factor (right image)

5.2.4.C Influence of parameter δ

The parameter δ is associated with the quadratic term on the momentum. It is associated with the stochastic noise in equation (5.12). In the next image we can see its influence on the momentum component of the metric, where we see that it controls the limit to which this components tends to. This limit is larger for large values of δ although it only grows with the square root of the parameter.

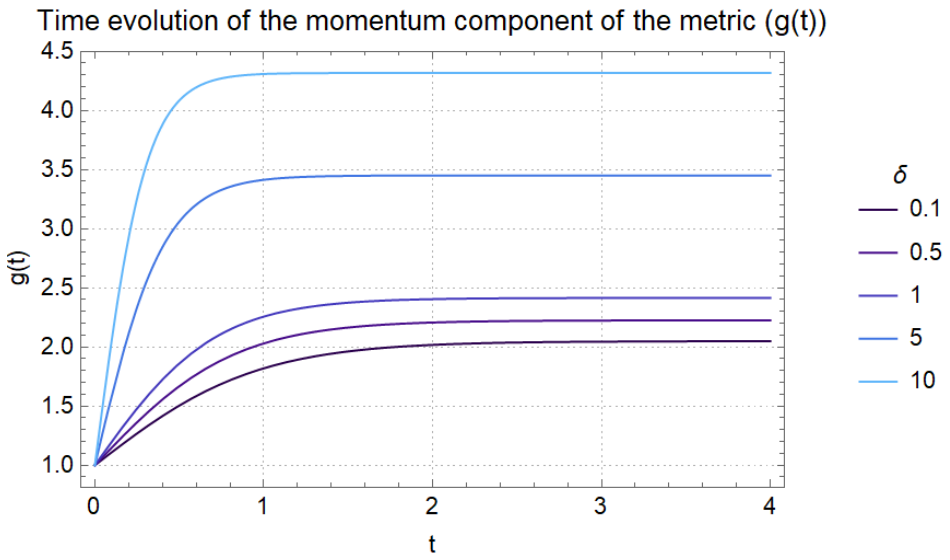

Figure 5.5: Momentum metric component g(t) for different values of δ where $\alpha = \beta = b = 1$

The role of δ on both the evolution of the center position and of the multiplicative factor is to regulate the decay present on the curve, the larger the value of δ the faster both curves tend to zero, as one can see on the below figure.

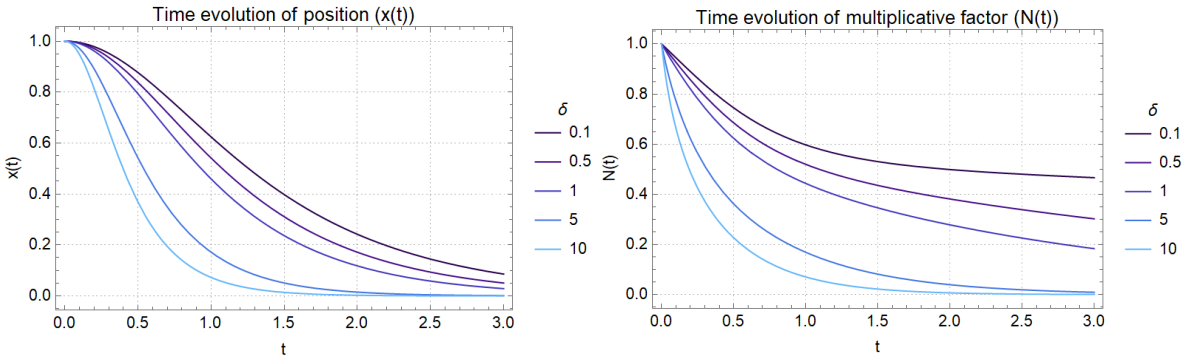

(a) Center's position x(t) for different values of δ where $\alpha = \beta = b = x_0 = 1$

(b) Multiplicative factor N(t) for different values of δ where $\alpha = \beta = b = x_0 = N_0 = \hbar = 1$

Figure 5.6: Influence of the parameter δ on the time evolution for position of the center of the wave packet (left image) and for the multiplicative factor (right image)

6

Conclusions and Future Work

The present work explores semiclassical dynamics of non-Hermitian Hamiltonians using a new methodological approach to simplify the equations of motion. We apply this methodology to analyze certain problems arising in control theory, where non-Hermitian operators arise.

Our starting point for the semiclassical analysis is the system of equations derived in Ref. [15], for the motion of a Wigner function on phase space. The Wigner function is of a coherent state for the harmonic oscillator. Specifically, the system of equations describes the motion of the center, the changes of the intrinsic metric of the coherent state and the variation of the parameter $\alpha(t)$, which is related to the total norm of the wave function. The anti Hermitian term induces a gradient flow that evolves the center towards the minima of the anti Hermitian term. At the same time, the norm of the wave function changes with time, which can be interpreted as absorption or dissipation of energy.

The semiclassical evolution of the center, the intrinsic metric of the coherent state and the parameter $\alpha(t)$, given by Eqs. (2.17), yields a set of $n^2/2 + 3n/2 + 1$ coupled differential equations, where n is the dimension of phase space. Using [24, 29] we introduced a new method of handling the system of equations consisting of complexifying the coordinates of the center of the Wigner function. This method reduces the problem into a simpler one, where the n equations for the center decouple from the rest of the dynamics. From the motion of the complexified center, one can then algebraically extract both the motion of the complex structure, which is related to the metric by Eq. (2.9), as well as the motion of the real center.

We studied several examples using both approaches of handling Eqs. (2.17). Namely, we considered the free particle in imaginary time, that is equivalent to the evolution under the heat equation. We also analyzed the harmonic oscillator in imaginary time, where an initial system is driven towards

the origin whilst the metric evolves to the trivial one, $G = \mathbb{1}$. For the latter case, we were only able to directly solve Eq. (2.17) for a specific choice of initial conditions, whereas the method developed in the present work of solving Eqs. (2.17) leads to solutions for the center and metric with generic initial conditions.

In the second part of the thesis, we applied our numerical method to propagate the time evolution of a wave function under non-Hermitian Hamiltonians. The method described is the split-step Fourier method, consisting on Trotter slicing the time evolution operator into several simpler operators that act diagonally either on position or on momentum space. We use a numerically effective Fourier transform to simply switch between the two representations. We then adapt the method to be able to propagate the time evolution of a Wigner function. This method was previously used in the literature for obtaining the Hermitian dynamics of both wave functions and Wigner distributions. Here, we generalize to the non-Hermitian case, which to our knowledge had not yet been done. We then test the developed method against Ref. [15] and corroborate the results therein.

Lastly, we applied our methods, both semiclassical and numerical, to stochastic optimization problems based in a connection between a class of stochastic differential equations and a Schrödinger-like equation introduced in Ref. [36]. This mapping makes naturally appear a non-Hermitian Hamiltonian. Furthermore, the value function, under this mapping, is obtained by taking the logarithm of the wave function. As such, by evolving the wave function we are also evolving the value function. As a specific example, we explore the harmonic oscillator originating from a particular stochastic optimization problem. We study how the choice of parameters of the problem affects the large time motion of initial localized states.

6.1 Future work

For future work, it would be interesting to try to develop a numerical method for performing the alternative method of decoupling the equations for the motion of the center and the metric of the initial Wigner function. With it, one could test the validity of the expectation that the proposed method may be, for non quadratic Hamiltonians, a better approximation than the one described in Eqs. (2.17).

One other avenue for further work is to further develop the numerical method described in chapter 4 to be able to handle Hamiltonians with cross terms, with both position and momentum operators. While these terms usually do not show up physical systems, we cannot rule them out of appearing on other applications of NHH, like the one described on chapter 5, where we do get a cross term.

Lastly, on the specific application of NHH explored on chapter 5, more work needs to be done in order to assess the usefulness of the NHH paradigm on the context of stochastic optimal control.

Bibliography

[1] Aoki, M. (1976). Stochastic control in economic theory and economic systems. *IEEE Transactions on Automatic Control*, 21(2):213–220.

[2] Bender, C. M. and Boettcher, S. (1998). Real spectra in non-hermitian hamiltonians having pt symmetry. *Physical Review Letters*, 80(24):5243–5246.

[3] Breuer, H. P. and Petruccione, F. (2002). *The theory of open quantum systems*. Oxford University Press, Great Clarendon Street.

[4] Cabrera, R., Bondar, D. I., Jacobs, K., and Rabitz, H. A. (2015). Efficient method to generate time evolution of the wigner function for open quantum systems. *Physical Review A*, 92(4).

[5] Case, W. B. (2008). Wigner functions and weyl transforms for pedestrians. *American Journal of Physics*, 76(10):937–946.

[6] Couto, C., Mourão, J. M., Nunes, J. P., and Ribeiro, P. (2020). Connecting stochastic optimization with schrödinger evolution with respect to non-hermitian hamiltonians. Article in preparation.

[7] Curtright, T. L. and Zachos, C. K. (2012). Quantum mechanics in phase space. *Asia Pacific Physics Newsletter*, 01(01):37–46.

[8] da Silva, A. (2004). *Lectures on Symplectic Geometry*. Lecture Notes in Mathematics. Springer Berlin Heidelberg.

[9] Dattoli, G., Torre, A., and Mignani, R. (1990). Non-hermitian evolution of two-level quantum systems. *Phys. Rev. A*, 42:1467–1475.

[10] El-Ganainy, R., Khajavikhan, M., Christodoulides, D., and Ozdemir, S. (2019). The dawn of non-hermitian optics. *Communications Physics*, 2.

[11] Fleming, W. and Soner, H. (2006). *Controlled Markov Processes and Viscosity Solutions*. Stochastic Modelling and Applied Probability. Springer New York.

[12] Ganguli, S. (1998). Quantum mechanics on phase space: Geometry and motion of the wigner distribution. Master's thesis.

[13] Glauber, R. J. (1963). Coherent and incoherent states of the radiation field. *Phys. Rev.*, 131:2766–2788.

[14] Graefe, E.-M., Höning, M., and Korsch, H. J. (2010). Classical limit of non-hermitian quantum dynamics—a generalized canonical structure. *Journal of Physics A: Mathematical and Theoretical*, 43(7):075306.

[15] Graefe, E.-M. and Schubert, R. (2011). Wave-packet evolution in non-hermitian quantum systems. *Physical Review A*, 83(6).

[16] Graefe, E.-M. and Schubert, R. (2012). Complexified coherent states and quantum evolution with non-hermitian hamiltonians. *Journal of Physics A: Mathematical and Theoretical*, 45(24):244033.

[17] Guo, A., Salamo, G. J., Duchesne, D., Morandotti, R., Volatier-Ravat, M., Aimez, V., Siviloglou, G. A., and Christodoulides, D. N. (2009). Observation of $\mathcal{PT}$-symmetry breaking in complex optical potentials. *Phys. Rev. Lett.*, 103:093902.

[18] Hall, B. C. (2015a). *The Baker–Campbell–Hausdorff Formula and Its Consequences*, pages 109–137. Springer International Publishing, Cham.

[19] Hall, B. C. (2015b). *The Matrix Exponential*, pages 31–48. Springer International Publishing, Cham.

[20] Hardin, R. (1973). Applications of the split-step fourier method to the numerical solution of nonlinear and variable coefficient wave equations. *SIAM Review (Chronicles)*, 15.

[21] Heiss, W. D. (2012). The physics of exceptional points. *Journal of Physics A: Mathematical and Theoretical*, 45(44):444016.

[22] Hunger, R. An introduction to complex differentials and complex differentiability.

[23] Kato, T. (2012). *Perturbation Theory for Linear Operators*. Classics in Mathematics. Springer Berlin Heidelberg.

[24] Kirwin, W. D., Mourão, J. M., and Nunes, J. P. (2013). Complex time evolution in geometric quantization and generalized coherent state transforms. *Journal of Functional Analysis*, 265(8):1460–1493.

[25] Kozii, V. and Fu, L. (2017). Non-hermitian topological theory of finite-lifetime quasiparticles: Prediction of bulk fermi arc due to exceptional point.

[26] Martinez Alvarez, V. M., Barrios Vargas, J. E., Berdakin, M., and Foa Torres, L. E. F. (2018). Topological states of non-hermitian systems. *The European Physical Journal Special Topics*, 227(12):1295–1308.

[27] Moiseyev, N. (2011). *Non-Hermitian Quantum Mechanics*. Cambridge University Press.

[28] Moroianu, A. (2007). *Lectures on Kähler Geometry*. London Mathematical Society Student Texts. Cambridge University Press.

[29] Mourão, J. M. and Nunes, J. P. (2015). On complexified analytic hamiltonian flows and geodesics on the space of kähler metrics. *International Mathematics Research Notices*, 2015(20):10624–10656.

[30] Nakahara, M. (2003). *Geometry, topology and physics*. CRC Press.

[31] Ozawa, T., Price, H. M., Amo, A., Goldman, N., Hafezi, M., Lu, L., Rechtsman, M. C., Schuster, D., Simon, J., Zilberberg, O., and et al. (2019). Topological photonics. *Reviews of Modern Physics*, 91(1).

[32] Perelomov, A. (1986). *Generalized Coherent States and Their Applications*. Springer-Verlag.

[33] Rosas-Ortiz, O. (2019). Coherent and squeezed states: Introductory review of basic notions, properties, and generalizations. *Integrability, Supersymmetry and Coherent States*, page 187–230.

[34] Stengel, R. (1994). *Optimal Control and Estimation*. Dover books on advanced mathematics. Dover Publications.

[35] Taha, T. R. and Ablowitz, M. I. (1984). Analytical and numerical aspects of certain nonlinear evolution equations. ii. numerical, nonlinear schrödinger equation. *Journal of Computational Physics*, 55(2):203 – 230.

[36] Theodorou, E., Buchli, J., and Schaal, S. (2010). A generalized path integral control approach to reinforcement learning. *Journal of Machine Learning Research*, 11(104):3137–3181.

[37] Whitney, D. and Junkel, E. (1982). Applying stochastic control theory to robot sensing, teaching, and long term control. *IFAC Proceedings Volumes*, 15(8):109 – 117. 4th IFAC/IFIP Symposium on Information Control problems in manufacturing Technology 1982, Maryland, USA, 26-28 October.

[38] Wigner, E. (1932). On the quantum correction for thermodynamic equilibrium. *Phys. Rev.*, 40:749–759.

A

Demonstration of the Weierstrass transform

The aim of this appendix is to show the following equivalence:

$$e^{t\frac{\partial^2}{\partial x^2}} f(x) = W_t[f(x)] \ , \tag{A.1}$$

where $W_t[f(x)]$ is called the generalized Weierstrass transform and is given by:

$$W_t[f(x)] = \frac{1}{\sqrt{4\pi}} \int_{-\infty}^{\infty} f(x-y) e^{-\frac{y^2}{4}} dy \ . \tag{A.2}$$

We note that $F(t,x) = e^{t\frac{\partial^2}{\partial x^2}} f(x)$ is the solution to the heat equation:

$$\frac{\partial f}{\partial t} = \frac{\partial^2 f}{\partial x^2} \ , \tag{A.3}$$

with boundary conditions $F(0,x) = f(x)$. As such, we can write $F(t,x)$ as a convolution of the initial boundary condition with the fundamental solution for the heat equation, i.e., with the Green's function for the heat equation, $G(t,x)$. This function is sometimes called the heat kernel and is given by:

$$G(t,x) = \left(\frac{1}{4\pi t}\right)^{\frac{1}{2}} e^{-x^2/4t} \ . \tag{A.4}$$

A general solution for the heat would have the following form:

$$F(t,x) = \int_{-\infty}^{\infty} dy f(y) G(t, x-y) \ . \tag{A.5}$$

We can check that the initial condition remains true due to the fact that as $t \to 0$, $G(t, x-y) \to \delta(x-y)$ which gives, after performing the integral, that $F(0,x) = g(x)$. Performing a change of variables on the last integral allows us to confirm that $F(x,t) = W_t[f(x)]$.

B

From the Fourier Transform to the Discrete Fourier Transform

The Fourier Transform of a function $f(x)$ is defined as:

$$\mathcal{F}\{f(x)\} := \tilde{f}(k) = \frac{1}{\sqrt{2\pi}} \int_{-\infty}^{\infty} dx f(x) e^{-ikx} \tag{B.1}$$

And its associated inverse transform is given by:

$$f(x) = \frac{1}{\sqrt{2\pi}} \int_{-\infty}^{\infty} dk \tilde{f}(k) e^{ikx} \tag{B.2}$$

If we assume that the function goes to zero at both ends, meaning the only relevant information is contained on the interval (a, b) then we can approximate the Fourier integral by a Riemann sum:

$$\tilde{f}(k) = \frac{1}{\sqrt{2\pi}} \sum_{n=0}^{N-1} f(x_n) e^{-ikx_n} \Delta x \ , \tag{B.3}$$

where $\Delta x = \frac{b-a}{N}$ and $x_n = a + n\Delta x$. If we discretize the momentum domain into $k = p\Delta k$ such that $\Delta x \Delta k = \frac{2\pi}{N}$ then we obtain:

$$\tilde{f}(p\Delta k) = \frac{1}{\sqrt{2\pi}} \Delta x e^{-ix_0 p\Delta k} \sum_{n=0}^{N-1} f(x_n) e^{-i2\pi np/N} = \sqrt{\frac{N}{2\pi}} \Delta x e^{-ix_0 p\Delta k} \tilde{f}_n \ , \tag{B.4}$$

which corresponds to having a phase factor multiplying the Discrete Fourier Transform of the sampled values of $f(x)$ here represented by the notation $\tilde{f}_n$.

Similarly for the inverse transform we obtain that:

$$f(x_n) = \frac{1}{\sqrt{2\pi}} \Delta k \sum_{p=0}^{N-1} \tilde{f}(k_p) e^{-i2\pi np/N} = \sqrt{\frac{N}{2\pi}} \Delta k f_n \ . \tag{B.5}$$

Notice that if we perform both the transformation and its inverse we get a factor $\frac{N}{2\pi} \Delta k \Delta x = 1$, due to our definition of Δk.

C

Fourier transform of the Wigner function

The Fourier transform of a position wave function $\psi(x)$ is given by:

$$\varphi(k) = \frac{1}{\sqrt{2\pi\hbar}} \int_{-\infty}^{\infty} dx e^{-ikx/\hbar} \psi(x) \ , \tag{C.1}$$

with the inverse transform being:

$$\psi(x) = \frac{1}{\sqrt{2\pi\hbar}} \int_{-\infty}^{\infty} dk \varphi(k) e^{ikx/\hbar} \ , \tag{C.2}$$

and its conjugate being:

$$\psi^*(x) = \frac{1}{\sqrt{2\pi\hbar}} \int_{-\infty}^{\infty} dk \varphi^*(k) e^{-ikx/\hbar} \ . \tag{C.3}$$

From Eq. (2.11) we can substitute the two inverse Fourier transforms to obtain:

$$\begin{aligned} W(x,p) &= \frac{1}{\pi\hbar} \frac{1}{2\pi\hbar} \int_{-\infty}^{\infty} dy \int_{-\infty}^{\infty} dk \int_{-\infty}^{\infty} dk' \varphi^*(k') \varphi(k) e^{2ipy/\hbar} e^{-ik'(x+y)/\hbar} e^{ik(x-y)/\hbar} = \\ &= \frac{1}{\pi\hbar} \frac{1}{2\pi\hbar} \int_{-\infty}^{\infty} dk \int_{-\infty}^{\infty} dk' \varphi^*(k') \varphi(k) e^{ix(k-k')/\hbar} \int_{-\infty}^{\infty} dy e^{i(2p-k-k')y/\hbar} \ . \end{aligned} \tag{C.4}$$

Noting that:

$$\int_{-\infty}^{\infty} dy e^{i(k-k')y\hbar} = 2\pi\delta(k-k') \ , \tag{C.5}$$

and that $\delta(a(x-x')) = \frac{1}{|a|}\delta(x-x')$, we can solve the integral in y and get:

$$\begin{aligned} W(x,p) &= \frac{1}{\pi\hbar} \int_{-\infty}^{\infty} dk \int_{-\infty}^{\infty} dk' \varphi^*(k') \varphi(k) e^{ix(k-k')/\hbar} \delta(2p-k-k') = \\ &= \frac{1}{\pi\hbar} \int_{-\infty}^{\infty} dk \varphi^*(2p-k) \varphi(k) e^{2ix(k-p)/\hbar} = \frac{1}{\pi\hbar} \int_{-\infty}^{\infty} dp' \varphi^*(p-p') \varphi(p+p') e^{2ixp'/\hbar} = \\ &= \frac{1}{\pi\hbar} \int_{-\infty}^{\infty} dp' \varphi^*(p+p') \varphi(p-p') e^{-2ixp'/\hbar} \ , \end{aligned} \tag{C.6}$$

where in the end we made the change of variables $p' = k - p$ and $p' \to -p'$.

D

Expression for the multiplicative factor

On this appendix is an expression for the multiplicative factor solution to the general case in Eq. (5.14):

$$N(t) = \sqrt[4]{b^2}\sqrt{2\alpha^2+2\beta\delta}\exp\left[\frac{1}{2}\left(\frac{2\left(\alpha t\hbar\left(b^2\left(2\alpha^2+\beta\delta\right)+\beta^2-2\alpha\beta b\right)+\beta\cosh\left(2t\sqrt{\alpha^2+\beta\delta}\right)\left(\alpha t\hbar\left(b^2\delta+2\alpha b-\beta\right)+b\mathsf{x0}^2(\beta-\alpha b)\right)-b^2\beta\mathsf{x0}^2\sqrt{\alpha^2+\beta\delta}\sinh\left(2t\sqrt{\alpha^2+\beta\delta}\right)+b\beta\mathsf{x0}^2(\alpha b-\beta)\right)}{\hbar\left(b^2\left(2\alpha^2+\beta\delta\right)+\beta\left(b^2\delta+2\alpha b-\beta\right)\cosh\left(2t\sqrt{\alpha^2+\beta\delta}\right)+\beta^2-2\alpha\beta b\right)}-\right.$$
$$\left.\tanh^{-1}\left(\frac{(\alpha+b\delta)\tanh\left(t\sqrt{\alpha^2+\beta\delta}\right)}{\sqrt{\alpha^2+\beta\delta}}\right)+\tanh^{-1}\left(\frac{(\alpha b-\beta)\tanh\left(t\sqrt{\alpha^2+\beta\delta}\right)}{b\sqrt{\alpha^2+\beta\delta}}\right)\right)\right]/$$
$$/\left(\sqrt[4]{b^2\left(2\alpha^2+\beta\delta\right)+\beta\left(b^2\delta+2\alpha b-\beta\right)\cosh\left(2t\sqrt{\alpha^2+\beta\delta}\right)+\beta^2-2\alpha\beta b}\sqrt[4]{2\alpha^2+\delta\left(b^2\delta+\beta\right)+2\alpha b\delta+\delta(\beta-b(2\alpha+b\delta))\cosh\left(2t\sqrt{\alpha^2+\beta\delta}\right)}\right)$$